
Astrometric and Geodetic Properties of Earth and the Solar System

Charles F. Yoder

1. BACKGROUND

The mass, size and shape of planets and their satellites and are essential information from which one can consider the balance of gravity and tensile strength, chemical makeup and such factors as internal temperature or porosity. Orbits and planetary rotation are also useful clues concerning origin, internal structure and tidal history. The tables compiled here include some of the latest results such as detection of densities of Pluto-Charon from analysis of HST images and the latest results for Venus' shape, gravity field and pole orientation based on Magellan spacecraft data. Data concerning prominent asteroids, comets and Sun are also included.

Most of the material here is presented as tables. They are preceded by brief explanations of the relevant geophysical and orbit parameters. More complete explanations can be found in any of several reference texts on geodesy [109, 74], geophysics [56, 58, 110] and celestial mechanics [13, 88, 98].

2. GRAVITY FIELD SHAPE AND INTERNAL STRUCTURE

External Gravity Field: The potential external of a non-spherical body [109, 57] at latitude ϕ and longitude λ and distance $r(\phi, \lambda) > R_e$ can be represented as a series with associated Legendre polynomials, $P_{nj}(\sin \phi)$,

C. Yoder, Jet Propulsion Laboratory, 183-501, 4800 Oak Grove Drive, Pasadena, CA 91109

Global Earth Physics
A Handbook of Physical Constants
AGU Reference Shelf 1

$$U = \frac{GM}{r} \sum_{n,j=0}^{n=\infty} \left(\frac{R_e}{r} \right)^n (C_{nj} \cos \lambda + S_{nj} \sin \lambda) P_{nj}, \quad (1)$$

and $j \leq n$. The zonal Legendre polynomials $P_{n0}(x)$ for $n < 7$ are

$$\begin{aligned} P_{00} &= 1 \\ P_{10} &= x \\ P_{20} &= (3x^2 - 1)/2 \\ P_{30} &= (5x^3 - 3x)/2 \\ P_{40} &= (35x^4 - 30x^2 + 3)/8 \\ P_{50} &= (63x^5 - 70x^3 + 15x)/8 \\ P_{60} &= (231x^6 - 315x^4 + 105x^2 - 5)/16. \end{aligned} \quad (2)$$

Higher order zonal functions can be derived from

$$P_{n0} = \frac{1}{2^n n!} \frac{d^n}{dx^n} (x^2 - 1)^n. \quad (3)$$

or from the recursion relation

$$(n+1)P_{n+1,0} = (2n+1)xP_{n,0} - nP_{n-1,0}. \quad (4)$$

The tesseral ($j < n$) and sectorial ($j = n$) functions can be deduced from

$$P_{nj} = \cos^j \phi \frac{d^j}{dx^j} P_{n0}. \quad (5)$$

Thus $P_{11} = \cos \phi$, $P_{21} = 3 \sin \phi \cos \phi$, $P_{22} = 3 \cos^2 \phi$, etc.

Surface topography can be expanded in similar fashion with $R_e C_{nm}^T$ and $R_e S_{nm}^T$ as coefficients of the respective Legendre functions.

Gravity Field Expansion Coefficients: The dimensionless gravity field coefficients $C_{nj} : S_{nj}$ of harmonic degree n and tesseral order j are related to the following volume integral.

$$(C_{nj} : S_{nj}) = \frac{(2 - \delta_{j0})}{MR_e^n} \frac{(n-j)!}{(n+j)!} \times \int dV \rho(\mathbf{r}) r^n P_{nj}(\sin \phi') (\cos j\lambda' : \sin j\lambda') \quad (6)$$

where ϕ^* and λ' are the latitude and longitude at internal position $\mathbf{r}(\phi', \lambda')$.

Both surface undulations and internal density variations contribute to the effective field. For an equivalent representation in terms of just density variations, then

$$\rho(\mathbf{r}) = \sum_{C,S,n,j} (\rho_{nj}^C(r) : \rho_{nj}^S(r)) \times P_{nj}(\sin \phi) (\cos j\theta : \sin j\theta), \quad (7)$$

and

$$(C_{nj} : S_{nj}) = \frac{4\pi}{MR_e^n(2n+1)} \int_0^{R_e} dr r^{n+2} \rho_{nj}^{C:S}(r). \quad (8)$$

A first order estimate of the contribution of *uncompensated* topography with radial harmonic coefficient C_{nj}^T to gravity is given by [12]

$$(C_{nj} : S_{nj}) = \frac{3}{(2n+1)} \frac{\rho_s}{\bar{\rho}} (C_{nj}^T : S_{nj}^T), \quad (9)$$

where ρ_s and $\bar{\rho}$ are the crustal and mean densities, respectively.

Airy compensation, where surface topography of a uniform density crust with average thickness H is compensated by bottom crustal topography, has external gravity which is smaller by a factor of $(1 - ((R_e - H)/R_e)^{n+2})$.

J_n : The usual convention for representation of the zonal coefficients is as J_n ,

$$J_n = -C_{n0}. \quad (10)$$

The *normalized* $\bar{C}_{nj} : \bar{S}_{nj}$ coefficients are

$$(\bar{C}_{nj} : \bar{S}_{nj}) = N_{nj} (C_{nj} : S_{nj}). \quad (11)$$

The normalization factor N_{nj} is

$$\begin{aligned} N_{nj}^2 &= \frac{1 + \delta_{j0}}{2} \int_{-\frac{\pi}{2}}^{\frac{\pi}{2}} \cos \phi d\phi P_{nj}^2 \\ &= \frac{(1 + \delta_{j0}) (n+j)!}{2(2n+1) (n-j)!} \end{aligned} \quad (12)$$

Kaula's Rule: The gravity field power spectra function σ_g for many solid planetary bodies tend to follow *Kaula's rule*,

$$\sigma_g = \sum_{n=0}^{\infty} \sum_{j=0}^{j=n} (\bar{C}_{nj}^2 + \bar{S}_{nj}^2) \simeq (2n+1) \frac{u^2}{n^q}, \quad (13)$$

where u is constant and q is $\simeq 4$. A similar scaling is found for topography with

$$\sigma_t \simeq \frac{t^2}{n(n+1)}. \quad (14)$$

and t a constant.

Moments of Inertia: The 2nd harmonic coefficients are related to the moments of inertia tensor I_{ij} where i and $j = 1, 2, 3$ correspond to the $\{x, y, z\}$ axes, respectively.

$$MR_e^2 C_{20} = - \left(C - \frac{1}{2}(B + A) \right), \quad (15)$$

$$MR_e^2 C_{21} = -I_{13}, \quad MR_e^2 S_{21} = -I_{23}, \quad (16)$$

$$MR_e^2 C_{22} = \frac{1}{4}(B - A), \quad (17)$$

where C , B and A are the principal moments about the z , y and x axes, respectively (that is, $C = I_{33}$, $B = I_{22}$ and $A = I_{11}$). The coordinate frame can be chosen such that the off-diagonal I_{ij} vanish and $C > B > A$ and is significant as it represents a minimum energy state for a rotating body. The choice for R_e is somewhat arbitrary, although the convention is to choose the equatorial radius. The moment for a uniform sphere is $\frac{2}{5}MR_e^2$, and if we wish to preserve the 2/5 coefficient for the mean moment $I = (A + B + C)/3$ for a triaxial ellipsoid, then $R_o = (a^2 + b^2 + c^2)/3$ is the appropriate choice. The volumetric mean radius $R_V = \sqrt[3]{abc}$ and differs from R_o in the second order.

The potential contributions from surface topography can be appreciated from a consideration of a uniform triaxial ellipsoid with surface defined by

$$\left(\frac{x}{a} \right)^2 + \left(\frac{y}{b} \right)^2 + \left(\frac{z}{c} \right)^2 = 1. \quad (18)$$

The harmonic coefficients and maximum principal moment for a triaxial ellipsoid with body axes $a > b > c$ and with *uniform density* are (to 4th degree)

$$C_{20} = \frac{1}{5R_o^2} \left(c^2 - \frac{1}{2}(a^2 + b^2) \right), \quad (19)$$

$$C_{22} = \frac{1}{20R_o^2} (b^2 - a^2), \quad (20)$$

$$C_{40} = \frac{15}{7} C_{20}^2, \quad (21)$$

$$C_{42} = \frac{15}{14} C_{20} C_{22}, \quad (22)$$

$$C_{44} = \frac{15}{49} C_{20} C_{22}, \quad (23)$$

$$C = \frac{1}{5} (a^2 + b^2) M = I - \frac{2}{3} M R_o^2 C_{20}. \quad (24)$$

while from symmetry the coefficients with either odd degree n or order j vanish.

Hydrostatic Shape: The hydrostatic shape [24, 18, 124] of a uniformly rotating body with rotation rate ω_s and radial density structure is controlled by the rotation parameter m and flattening f ,

$$m \equiv \frac{\omega_s^2 a^3}{GM}, \quad f = \frac{a - b}{a}. \quad (25)$$

Other choices for the spin factor which appear in the literature are $m_v = \omega_s^2 b a^2 / GM = m(1 - f)$, $m_o = \omega_s^2 R_o^3 / GM \simeq m_v(1 - \frac{2}{3}f^2)$ and $m_g = \omega_s^2 a / g_e$. The ellipticity $\hat{e} = \sqrt{1 - (b/a)^2}$ is sometimes used instead of f .

The relationship between J_2 , J_4 and f ($\tilde{f} = f(1 - \frac{1}{2}f)$ and $\tilde{m}_v = m_v(1 - \frac{2}{7}f)$) is [24]

$$J_2 \simeq \frac{1}{3} \left(2\tilde{f} - \tilde{m}_v + \frac{11}{49} mf^2 \right), \quad (26)$$

$$J_4 \simeq -\frac{15}{7} J_2^2 + \frac{5}{21} \left(\frac{4}{5} \tilde{f} - \tilde{m}_v \right)^2. \quad (27)$$

An expression for the hydrostatic flattening, accurate to second order, is [50]

$$f = \frac{1}{2} (m_v + 3J_2) \left(1 + \frac{3}{2} J_2 \right) + \frac{5}{8} J_4. \quad (28)$$

The mean moment of inertia for a fluid planet is also related to f and m through an approximate solution to Clairaut's equation.

$$x \frac{d\eta}{dx} - \eta^2 + \left(\frac{\rho}{\rho_o} - 5 \right) \eta = 6 \left(\frac{\rho}{\rho_o} - 1 \right) \quad (29)$$

where $\eta = d \ln f(x) / d \ln x$ is the logarithmic derivative of the flattening, and $\rho_o(x) = 3g(x)/4\pi x$ is the mean density inside radius x , and is proportional to gravity $g(x)$. The solution of (29) results in a relationship between f , m and the mean moment of inertia I which is only weakly dependent on the actual density profile for solid bodies.

$$I \simeq \frac{2}{3} M R_o^2 \left[1 - \frac{2}{5} \left(\frac{1}{1 + \delta_1} \right) \sqrt{\frac{5m_v}{2f} - 1 + \delta_2} \right], \quad (30)$$

$$\delta_2 \simeq \frac{3}{7} f + \left(\frac{5m_v}{2f} - 2 \right) \left(\frac{8m_v - 3f}{42} \right), \quad (31)$$

$$\delta_1 = \frac{\int_0^{R_o} x^3 g(x) \bar{\psi}(\eta) dx}{\int_0^{R_o} x^3 g(x) dx}, \quad (32)$$

$$\bar{\psi}(\eta) = \frac{1 + \frac{1}{2}\eta - \frac{1}{10}\eta^2 - \sqrt{1 + \eta}}{\sqrt{1 + \eta}}. \quad (33)$$

Both δ_1 and δ_2 are small for terrestrial planets (e.g. $-0.0005 \leq \delta_1 \leq 0.0008$ and $0.48m \leq \delta_2 \leq 0.8m$). For Earth, $\delta_1 = -0.00040$ and $\delta_2 = 0.49m$. The above relationships connecting f , m_v , and J_2 appear to be self-consistent for the giant planets though significant surface zonal winds are observed. However, the factor δ_1 can be relatively large ($0.05 < \delta_1 < 0.08$) for a variety of plausible giant planet interior models [51], such that (30) provides an upper bound on $I/M R^2$ for $\delta_1 = 0$.

A satellite's shape is also influenced by secular tides raised by the planet. The spin factor is augmented by the factor $\left[1 + \frac{3}{2} (n/\omega_s)^2 (1 - \frac{3}{2} \sin^2 \epsilon) \right]$ for non-synchronous rotation. Here n is orbital mean motion, ω_s is satellite spin rate and ϵ is satellite inclination of its equator to the orbit. Most satellites have synchronous rotation for which the hydrostatic shape is triaxial. The expected value for the ratio $(b-c)/(a-c)$ is 1/4 for small m [20, 30]. A first order solution relating the flattening $f_1 = (a-c)/a$, gravity factor $J^1 = J_2 + 2C_{22}$ and spin $m_1 = 4m$ is obtained by replacing these factors (i.e. $f \rightarrow f_1$, $J_2 \rightarrow J^1$ and $m \rightarrow m_1$) in (26).

Surface Gravity: The radial component of surface gravity $g(r, \phi)$ for a uniformly rotating fluid body is

$$g = \frac{GM}{r^2} \left(1 + \frac{3}{2} J_2 \left(\frac{a}{r} \right)^2 (1 - 3 \sin^2 \phi) \right) \quad (34)$$

$$-m \left(\frac{r}{a} \right)^3 \cos^2 \phi. \quad (35)$$

The equatorial gravity is

$$g_e = g(a, 0) = \frac{GM}{a^2} \left(1 + \frac{3}{2} J_2 - m \right), \quad (36)$$

while the polar gravity is

$$g_p = \frac{GM}{b^2} \left(1 - 3 \left(\frac{a}{b} \right)^2 J_2 \right). \quad (37)$$

Geodetic Latitude: The geodetic (or geographic) latitude ϕ' measures the angle formed by the surface normal vector on the plane of the equator and is related to the geocentric latitude ϕ by (see Figure 1)

$$\tan \phi' = \left(\frac{b}{a} \right)^2 \tan \phi = (1 - f)^2 \tan \phi. \quad (38)$$

An expansion for the difference angle is

$$\phi - \phi' \simeq \hat{f} \sin 2\phi' (1 - 2\hat{f} \sin^2 \phi'), \quad (39)$$

where

$$\hat{f} = f(1 - \frac{1}{2}f)/(1 - f)^2. \quad (40)$$

Normal gravity to the ellipsoid is [74]

$$g = \frac{ag_e \cos^2 \phi' + bg_p \sin^2 \phi'}{\sqrt{a^2 \cos^2 \phi' + b^2 \sin^2 \phi'}}. \quad (41)$$

3. ORBITS AND THEIR ORIENTATIONS

Orbits of all planets and satellites are slightly elliptical in shape where the orbit focus lies at the primary center of mass and is displaced from the ellipse center of figure by ea , where e is the orbit *eccentricity* and a is the *semimajor axis*. The ratio of minor to major axes of the orbit ellipse is $\sqrt{1 - e^2}$. The rate that area is swept out relative to the focus is governed by the Keplerian condition $r^2 \frac{d}{dt} f \simeq \text{constant}$ where the angle f (true anomaly) is measured relative to the minimum separation or pericenter. The mean motion $n = \frac{d}{dt}(\ell + \omega + \Omega)$ and the orbital period is $2\pi/n$. The radial position is governed by the following two relations which connect the radial separation r , semimajor axis a , eccentricity e , true anomaly f and mean anomaly ℓ (which varies linearly with time for the strictly two body case),

$$r = \frac{a(1 - e^2)}{1 + e \cos f}; \sin(\ell + \frac{er \sin f}{a\sqrt{1 - e^2}}) = \frac{r \sin f}{a\sqrt{1 - e^2}}. \quad (42)$$

If f is known, then r and ℓ are found directly. On the other hand, if ℓ (or the time relative to perihelion passage) is known, then f and r can be obtained by iteration. An alternative is to employ the eccentric anomaly E which is directly connected to f and ℓ .

$$\tan \frac{1}{2}f = \sqrt{\frac{1+e}{1-e}} \tan \frac{1}{2}E, \quad (43)$$

$$\ell = E - e \sin E, \quad (44)$$

$$r = a(1 - e \cos E). \quad (45)$$

The eccentric anomaly E measures the angular position relative to the ellipse center.

For small e , the equation of center is [88]

$$f - \ell \simeq e(2 - \frac{1}{4}e^2) \sin \ell + \frac{5}{4}e^2 \sin 2\ell + \frac{13}{12}e^3 \sin 3\ell. \quad (46)$$

Similar expansions of a/r and r/a in terms of the mean anomaly are

$$\frac{a}{r} = 1 + e(1 - \frac{1}{8}e^2) \cos \ell + e^2 \cos 2\ell + \frac{9}{8}e^3 \cos 3\ell, \quad (47)$$

$$\frac{r}{a} = 1 + \frac{1}{2}e^2 - e(1 - \frac{3}{8}e^2) \cos \ell - \frac{1}{2}e^2 \cos 2\ell - \frac{3}{8}e^3 \cos 3\ell \quad (48)$$

The natural $\{x, y, z\}$ coordinates of the orbit which lie in the $\{x, y\}$ plane are

$$\mathbf{r} = \begin{bmatrix} r \cos(f + \omega) \\ r \sin(f + \omega) \\ 0 \end{bmatrix} \quad (49)$$

The spatial orientation of an orbit relative to the ecliptic and equinox is specified by three Euler angles: longitude of the ascending node Ω describing the position of the intersection line relative to a fixed point on the ecliptic, argument of perihelion ω measured from the node to the pericenter and orbit inclination I . The $\{x, y, z\}$ coordinates in this frame are

$$\frac{\mathbf{r}_e}{r} = \begin{bmatrix} \cos(f + \omega) \cos \Omega - \cos I \sin(f + \omega) \sin \Omega \\ \cos(f + \omega) \sin \Omega + \cos I \sin(f + \omega) \cos \Omega \\ \sin I \sin(f + \omega) \end{bmatrix} \quad (50)$$

The ecliptic spherical coordinates (longitude ψ and latitude β) of the position vector \mathbf{r}_e are defined by

$$\begin{bmatrix} x_e \\ y_e \\ z_e \end{bmatrix} = \begin{bmatrix} \cos \psi \cos \beta \\ r \sin \psi \cos \beta \\ r \sin \beta \end{bmatrix} \quad (51)$$

The $\{x, y, z\}$ planetary, orbital coordinates relative to an angular, *equatorial* coordinate frame centered in the sun depend on earth's obliquity ϵ and are

$$\mathbf{r}_g = \mathbf{R}\mathbf{r}. \quad (52)$$

The rotation matrix \mathbf{R} , by column, is

$$\mathbf{R}_1 = \begin{bmatrix} \cos \Omega \\ \cos \epsilon \sin \Omega \\ \sin \epsilon \sin \Omega \end{bmatrix}, \quad (53)$$

$$\mathbf{R}_2 = \begin{bmatrix} -\cos I \sin \Omega \\ \cos \epsilon \cos I \cos \Omega - \sin \epsilon \sin I \\ \sin \epsilon \cos I \cos \Omega + \cos \epsilon \sin I \end{bmatrix}, \quad (54)$$

$$\mathbf{R}_3 = \begin{bmatrix} \sin I \sin \Omega \\ -\cos \epsilon \sin I \cos \Omega - \sin \epsilon \cos I \\ -\sin \epsilon \sin I \cos \Omega + \cos \epsilon \cos I \end{bmatrix} \quad (55)$$

The geocentric position \mathbf{r}'_g of a planet (still in equatorial coordinates) is given by

$$\mathbf{r}'_g = \mathbf{r}_g + \mathbf{r}_\odot \quad (56)$$

where \mathbf{r}_\odot points from earth towards sun and \mathbf{r}_g points from sun towards planet.

R.A. and Dec.: The *right ascension* α and *declination*

nation δ of an object relative to earth's equator and equinox (see Figure 2) are related to the components of \mathbf{r}'_g by

$$\begin{aligned} x'_g &= r \cos \alpha \cos \delta \\ y'_g &= r \sin \alpha \cos \delta \\ z'_g &= r \sin \delta \end{aligned} \quad (57)$$

If a translation is unnecessary, as with planetary poles of rotation or distant objects, then (57) can be used to relate the orbital elements to α and δ . The equatorial and ecliptic coordinates are related by

$$\mathbf{r}_e = \begin{bmatrix} 1 & 0 & 0 \\ 0 & \cos \epsilon & \sin \epsilon \\ 0 & -\sin \epsilon & \cos \epsilon \end{bmatrix} \mathbf{r}_g \quad (58)$$

Kepler's Third Law: $GM_t = n^2 a^3$ ($M_t = M_{\text{planet}} + M_{\text{satellite}}$) for satellite orbits is modified by zonal planetary gravity, other satellites and Sun. The lowest order expression is [82, 79]

$$\begin{aligned} N^2 A^3 = GM_t \left(1 + \frac{3}{2} J_2 \left(\frac{R_e}{a} \right)^2 - \frac{15}{8} J_4 \left(\frac{R_e}{a} \right)^2 \right. \\ \left. - \frac{1}{2} \left(\frac{n_\odot}{N} \right)^2 \left(1 - \frac{3}{2} \sin^2 \epsilon \right) + P \right), \end{aligned} \quad (59)$$

$$\begin{aligned} P = \frac{1}{2} \sum_j S_j \frac{M_j}{M_p} \frac{a}{a_>} \frac{1}{(1 - \alpha_j^2)} \times \\ \left([(1 + S_j)(1 - \alpha_j^2) + 2\alpha_j^2] b_{1/2}^0(\alpha_j) - 2\alpha_j b_{1/2}^1(\alpha_j) \right). \end{aligned} \quad (60)$$

where N and A are the *observed* mean motion and semimajor axis, respectively and ϵ is the planetary obliquity to its orbit. The orbital period is $2\pi/N$. The sum P gives the contributions from all other satellites of mass M_j and depends on *Laplace coefficients* $b_{1/2}^0(\alpha)$ and $b_{1/2}^1(\alpha)$ which in turn can be expressed as a series [88, 13] in $\alpha = a_</a_>$. For a given pair, $a_<$ and $a_>$ are the semimajor axes of the interior and exterior satellites, respectively. The factor $S_j = 1$ if $a < a_j$ and $S_j = -1$ if $a > a_j$.

Laplace Coefficients: The expansion of the function $\Delta^{-s} = (1 + \alpha^2 - 2\alpha \cos x)^{-s}$ is

$$\Delta^{-s} = \frac{1}{2} b_s^0 + \sum_{j=1}^{\infty} b_s^j \cos jx. \quad (61)$$

The general coefficient $b_s^j(\alpha)$ is

$$\begin{aligned} b_s^j(\alpha) &= \frac{2}{\pi} \int_0^\pi dx \cos jx (1 + \alpha^2 - 2\alpha \cos x)^{-s} \\ &= 2\alpha^j \frac{\Gamma(s+j)}{\Gamma(s)\Gamma(j+1)} \sum_q C_{jsq} \alpha^{2q}, \end{aligned} \quad (62)$$

$$C_{jsq} = \left(\frac{\Gamma(s+q)\Gamma(s+j+q)\Gamma(j+1)}{\Gamma(s)\Gamma(s+j)\Gamma(I+1+q)\Gamma(q+1)} \right) \quad (63)$$

$\Gamma(x) = (x-1)\Gamma(x-1)$ is the Gamma function. Also, $\Gamma(1) = 1$ and $\Gamma(1/2) = \sqrt{\pi}$.

Apsidal and Nodal Precession: The satellite node and argument of periapse also precess and the lowest order expressions are [82] ($\tilde{\omega} = \omega + \Omega$)

$$\begin{aligned} \frac{d}{dt} \tilde{\omega} \simeq & \frac{3}{2} N \left(\frac{R_e}{A} \right)^2 \left(J_2 - \frac{5}{2} J_4 \left(\frac{R_e}{A} \right)^2 - \frac{3}{4} J_2^2 \right) + \\ & \frac{3}{4} \left(\frac{n_\odot}{N} \right)^2 \left(2 - \cos \epsilon - \frac{5}{2} \sin^2 \epsilon \right) + N \bar{P} \end{aligned} \quad (64)$$

$$\begin{aligned} \frac{d}{dt} \Omega \simeq & -\frac{3}{2} N \left(\frac{R_e}{A} \right)^2 \left(J_2 - \frac{5}{2} J_4 \left(\frac{R_e}{A} \right)^2 - \frac{9}{4} J_2^2 \right) - \\ & \frac{3}{4} \left(\frac{n_\odot}{N} \right)^2 \left(1 - \frac{3}{2} \sin^2 \epsilon \right) - N \bar{P}. \end{aligned} \quad (65)$$

Here \bar{P} is the contribution from other satellites and is

$$\bar{P} = \frac{1}{4} \sum_j \frac{M_j}{M_p} \frac{a}{a_>} \alpha_j b_{3/2}^1(\alpha_j) \quad (66)$$

$$\simeq \frac{3}{4} \sum_j \frac{M_j}{M_p} \frac{a}{a_>} \alpha_j^2 \left(1 + \frac{15}{8} \alpha_j^2 \right). \quad (67)$$

Invariable Plane: The action of the sun causes satellites to precess about the normal to the invariable plane (also known as the Laplacian plane), which is inclined by i to the planetary equator, and defined to lowest order by

$$2J_2 \sin(2i) = \left(\frac{n_\odot}{N} \right)^2 (1 - e^2)^{-1/2} \sin 2(\epsilon - i). \quad (68)$$

The invariable plane normal vector lies between the planetary spin vector and planetary orbit normal and the three normals are coplanar.

Planetary Precession: The precession of a planet's spin axis (if we ignore the variations induced by the motion of planetary orbit plane [64]) resulting from the sun and its own satellites is given by [98]

$$\begin{aligned} \frac{d}{dt} \phi = -\frac{3}{2} \frac{MR_e^2}{C\omega_s} J_2 n_\odot^2 \times \\ \left(\cos \epsilon + \sum_j \left(\frac{n_j}{n_\odot} \right)^2 \frac{M_j}{M_j + M} \cos(\epsilon - i_j) \right), \end{aligned} \quad (69)$$

where C is the polar moment of inertia and ω_s is the planet spin rate. Numerical modeling of the long term behavior of the obliquity of terrestrial planets [64, 112] indicate that their orientation (especially Mars) is at some time in their histories chaotic.

Cassini State: The mean orientation of a synchronously locked satellite is described by three laws:

6 ASTROMETRIC AND GEODETIC DATA

The same side of the moon faces the planet. The satellite's rotation axis lies in the plane formed by the orbit normal and invariable plane normal. The lunar obliquity is constant.

The lunar obliquity relative to its orbit ϵ_s , depends of the satellite precession rate $\frac{d}{dt}\Omega$ in addition to the moments of inertia [87].

$$\begin{aligned} \frac{d}{dt}\Omega \sin(\epsilon_s - I) = & -\frac{3}{2} \sin \epsilon_s \left(\frac{C-A}{C} \cos \epsilon_s \right. \\ & \left. + \frac{1}{4} \frac{B-A}{C} \sin^2 \frac{1}{2} \epsilon_s \right). \end{aligned} \quad (70)$$

4. DYNAMICAL CONSTRAINTS

A few simple parameters are defined here which are useful in determining dynamical characteristics of planets and satellites.

Escape Velocity v_∞ and Minimum Orbit Velocity v_o : The minimum velocity to orbit just above the surface of an airless spherical body of mass M and radius R is v_o while the minimum velocity necessary for an object to just reach infinity is v_∞ .

$$v_o = \sqrt{\frac{GM}{R}} = \sqrt{gR}, \quad (71)$$

$$v_\infty = \sqrt{2}v_o = 118.2 \left(\frac{R}{100\text{km}} \right) \left(\frac{\bar{\rho}}{2.5 \text{ g cm}^{-3}} \right)^{1/2} \text{ m s}^{-1}.$$

Hills' Sphere: A roughly spherical volume about a secondary body in which a particle *may* move in bounded motion, at least temporarily. The Hills' radius h is proportional to the cube root of the mass ratio M_s/M_p of satellite to planet.

$$h = \kappa a \left(\frac{M_s}{3M_p} \right)^{1/3} = \kappa R_s \frac{a}{R_p} \left(\frac{\rho_s}{3\rho_p} \right)^{1/3}. \quad (72)$$

where $\kappa \leq 1$. This factor also reduces the effective escape velocity by a factor of $\sim \sqrt{1 - R_s/h}$.

Roche Limit: A fluid satellite can be gravitationally disrupted by a planet if its Hills' radius is smaller than the satellite's mean radius of figure, R_s . That is, for $R_s \leq h$, a particle will move off the satellite at the sub- and anti-planet positions (orbit radius $A \leq 1.44R_p(\rho_p/\rho_s)^{1/3}$), and defines a minimum orbital radius inside which satellite accretion from ring material is impeded. The Darwin condition where a fluid body begins to fill its Roche lobe is less stringent and is [20]

$$A_{\text{Roche}} = 2.455 R_p \left(\frac{\rho_p}{\rho_s} \right)^{1/3}. \quad (73)$$

5. TIDES AND TIDAL FRICTION

Love Numbers: The elastic deformation of a satellite due to either a tide raised by the planet or deformation caused a satellite's own rotation is set by the dimensionless Love number k_2 . The corresponding changes in the moment of inertia tensor are

$$\delta I_{ij}(\text{tides}) = -\frac{k_2 M_p R_s^5}{r^3} \left(u_i u_j - \frac{1}{3} \delta_{ij} \right), \quad (74)$$

$$\delta I_{ij}(\text{spin}) = \frac{1}{3} \frac{R_s^5}{GM_s} \omega_i \omega_j \left(k_2 - \left(\frac{1}{3} k_2 - \frac{1}{2} n_o \right) \delta_{ij} \right). \quad (75)$$

Here u_i are the direction cosines of the tide-raising satellite as seen from the satellite's body-fixed reference system (i.e. $u_i = r_i/r$), while ω_i are the Cartesian components of the spin vector.

The Love number $k_2 \simeq 3/2/(1 + 19\mu/\rho g R)$ for small homogeneous satellites. An appropriate rigidity μ for rocky satellites is $\sim 5 \times 10^{11}$ dyne-cm $^{-2}$ for rocky bodies and $\sim 4 \times 10^{10}$ dyne-cm $^{-2}$ for icy bodies. Fluid cores can substantially increase k_2 . For fluid planets, the equivalent hydrostatic $k_2(\text{fluid}) = 3J_2/m$ is appropriate, where $m = \omega_s^2 R^3/GM$ is the rotation factor defined earlier in equation (25).

The term proportional to n_o arises from a purely radial distortion and depends on the bulk modulus, K . An expression for n_o has been derived for a uniform spherical body [120].

$$n_o = \frac{32}{105} \left(\frac{\rho g R}{K + \frac{4}{9}\mu} \right) \left(1 + \frac{14}{15} \frac{\mu}{K} \right). \quad (76)$$

Typically, $K \sim \frac{5}{3}\mu$ and thus $n_o \sim k_2$ for small satellites.

The surficial tidal deformation $\mathbf{d}(\mathbf{R}')$ of the satellite at a point \mathbf{R}' depends on the interior angle θ subtending the surface \mathbf{R}' and satellite \mathbf{r} position vectors [62]. Its magnitude is set by two additional Love numbers h_2 and l_2 . Also, $h_2 \simeq \frac{5}{3}k_2$ and $l_2 \simeq \frac{1}{2}k_2$ for small objects.

$$\mathbf{d} = \frac{GM_p R}{g_s r^3} \left(h_2 \mathbf{R}' P_{20}(\cos \theta) - 3l_2 \hat{\theta} \mathbf{R}' \sin \theta \cos \theta \right), \quad (77)$$

where g_s is satellite gravity and $\hat{\theta}$ is a unit vector, normal to \mathbf{R}' and pointing from \mathbf{R}' toward \mathbf{r} .

Tidal Acceleration and Spin Down: The tidal acceleration of a satellite caused by the inelastic tide it raises on a planet with rotation rate ω_p is given by

$$\frac{d}{dt}n \simeq -\frac{9}{2} \frac{k_{2p}}{Q_p} \frac{M_s}{M_p} \left(\frac{R_p}{a} \right)^5 n^2 \text{sgn}(\omega_p - n), \quad (78)$$

with a and n are semimajor axis and mean motion, respectively. The planetary dissipation factor $Q_p \propto 1/(\text{tidal phase lag})$ is defined by

$$Q^{-1} = \frac{1}{2\pi} \frac{\Delta E}{E_e}, \quad (79)$$

where E_e is the elastic distortion energy and ΔE is the energy dissipated during one flexing cycle. The rate that a satellite's own spin changes toward synchronous rate due to the inelastic tide that the planet raises on the satellite is

$$\frac{d}{dt}\omega_s \simeq -\frac{3}{2} \frac{k_{2s}}{Q_s} \frac{M_p R_s^2}{C_s} \left(\frac{R_s}{a} \right)^3 \frac{n^2}{\omega_s} \text{sgn}(\omega_s - n), \quad (80)$$

where C_s is the satellite's principal moment of inertia. The contribution of a satellite to the despinning of a planet is

$$\frac{d}{dt}\omega_p \simeq -\frac{3}{2} \frac{k_{2p}}{Q_p} \frac{M_s R_p^2}{C_p} \left(\frac{R_p}{a} \right)^3 \frac{n^2}{\omega_p} \text{sgn}(\omega_p - n), \quad (81)$$

Wobble Period and Damping Rate: The free Eulerian nutation period T_w of a rigid triaxial body (which for earth is known as the Chandler wobble) is [62]

$$T_w = \frac{2\pi}{\omega_s} \sqrt{\frac{AB}{(C-A)(C-B)}} \quad (82)$$

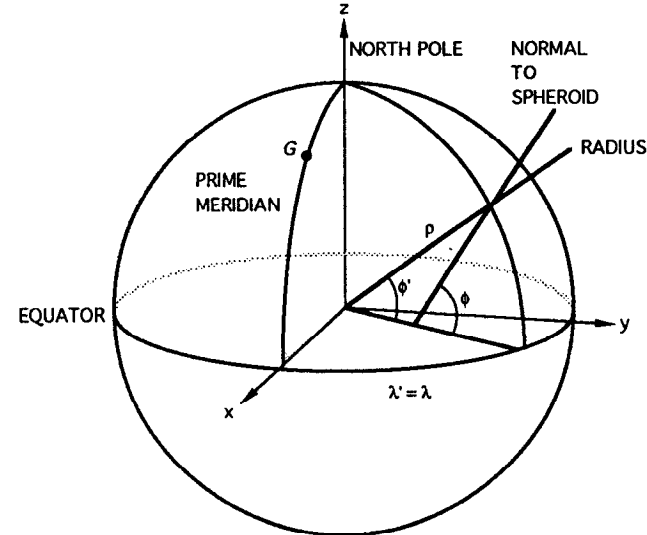


Fig. 1. Spheroidal coordinate system.

if the object's spin is *not* locked in a spin-orbit resonance. The gravitational torque exerted by a planet a satellite's figure decreases the wobble period by the factor D^{-1} , where

$$D^2 = D_1 D_2 \quad (83)$$

and

$$D_1 = 1 + \frac{3}{2}(1 - \delta_{n,\omega_s}) \left(\frac{n}{\omega_s} \right)^2, \quad (84)$$

$$D_2 = 1 + \frac{3}{2}(1 + \delta_{n,\omega_s}) \left(\frac{n}{\omega_s} \right)^2. \quad (85)$$

The function $\delta_{n,\omega_s} = 1$ if satellite rotation is synchronous (i.e. $\omega_s = n$) and zero otherwise [12, 118]. For a body with a fluid core, the moments of inertia $C > B > A$ are of the mantle only. Finally, the elasticity of a body increases the period by a factor of $\simeq J_2/(J_2 - \frac{1}{3}k_2 m)$.

The wobble damping time scale τ_w is

$$\tau_w^{-1} \simeq \frac{1}{3} \omega_s m \frac{k_2}{Q_w} \frac{M_s R_s^2}{C_s} F(\alpha, \beta). \quad (86)$$

The function F is of order unity and depends on the moment differences, $\alpha = (C-B)/B$ and $\beta = (C-A)/B$. For non-synchronous rotation, the explicit expression is [118]

$$F = \left(1 + \frac{3}{2} \left(\frac{n}{\omega_s} \right)^2 \right)^2 \frac{1 + \sqrt{\frac{\alpha}{\beta}}}{\sqrt{\frac{\beta}{\alpha}} + \sqrt{\frac{\alpha}{\beta}}} \quad (87)$$

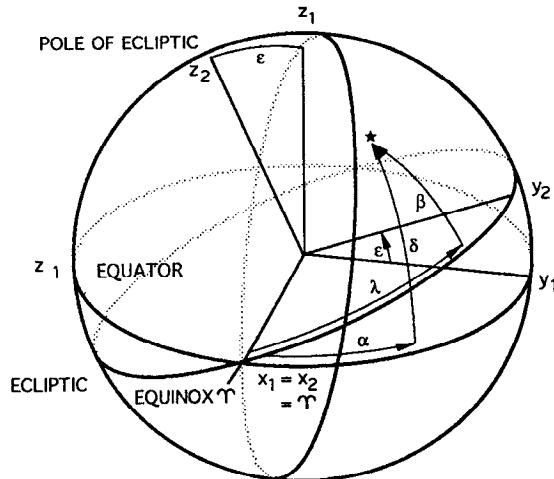


Fig. 2. Angular location of distant object relative to equatorial (α, δ) and ecliptic (ψ, β) reference planes. Equinox origin is known as the first point of Aries.

Table 1. Basic Astronomical Constants

Time units	
Julian day	$d = 86400 \text{ s}$
Julian year	$\text{yr} = 365.25 \text{ d}$
Julian Century	$\text{Cy} = 36525 \text{ d}$
Tropical year (equinox to equinox)	365.2421897 d
Sidereal (quasar reference frame)	365.25636 d
Anomalistic year (apse to apse)	365.25964 d
Mean sidereal day	$23^{\text{h}}56^{\text{m}}04^{\text{s}}09054$ 86164.09054 s
Defining constants	
Speed of light	$c \equiv 299792458 \text{ m s}^{-1}$
Gaussian constant	$k \equiv 0.01720209895$
Derived constants	
Light time for 1 AU: τ_A	499.00478370 s
Astronomical unit distance $\mathbf{AU} = c\tau_A$	$1.495978706(6 \pm 5) \times 10^{11} \text{ m}$
Gravitational constant: \mathbf{G}	$6.672(59 \pm 84) \times 10^{-11} \text{ kg}^{-1} \text{ m}^3 \text{ s}^{-2}$
Solar $GM_{\odot} = k^2 AU^3 d^{-2}$	$1.327124399(4 \pm 3) \times 10^{20} \text{ m}^3 \text{ s}^{-2}$
Solar parallax $\pi_0 = \sin^{-1}(a_e/AU)$	$8.^{\prime\prime}794144$
Constant of aberration (J2000)	$\kappa = 20.^{\prime\prime}49552$
Earth-Moon mass ratio	$81.3005(87 \pm 49)$
Obliquity of ecliptic (J2000)	$\epsilon = 23^{\circ}26'21''4119$
General precession in longitude	$5029.^{\prime\prime}0966 \text{ Cy}^{-1}$
IAU(1976) values	
Light time for 1 AU: τ_A	499.004782 s
Astronomical unit distance \mathbf{AU}	$1.49597870 \times 10^{11} \text{ m}$

Table 1: Notes: Modern planetary ephemerides such as DE 200 [103] determine the primary distance scale factor, the astronomical unit (AU). This unit is the most accurate astrometric parameter, with an estimated uncertainty of $\pm 50\text{m}$ (Standish, priv. comm.). Lunar laser ranging and lunar orbiter Doppler data determine the earth-moon mass ratio [38][32]. The (IAU,1976) system [95].

Table 2. Earth: Geodetic and Geophysical Data

Mass	$5.9736 \times 10^{24} \text{ kg}$
Mean radius R_V ¹	$6371.01 \pm 0.02 \text{ km}$
Density	5.515 g cm^{-3}
Equatorial radius	
(IAU,1976)	$a = 6378140 \text{ m}$
(Geod. ref. sys., 1980) ²	$a = 6378137 \text{ m}$
(Merit,1983)	$a = 6378136 \text{ m}$
Flattening $f = (a - b)/a$	
(IAU,1976; Merit)	$1/298.257$
(G.R.S.,1980)	$1/298.257222$
Polar axis: $b = a(1 - f)$ ²	6356.752 km
Gravity J_2 coeff.	
(IAU,1976)	0.00108263
(GEM T2,1990) ³	0.0010826265
$C_{22} (\times 10^{-6})$	1.5744
$S_{22} (\times 10^{-6})$	-0.9038
$(B - A)/Ma^2 (\times 10^{-6})$	7.2615
Longitude of axis a	$14.9285^{\circ} \text{ E}$
Surface gravity ²	
$g_p \text{ (m s}^{-2}\text{)}$	9.8321863685
g_e	9.7803267715
$g_o = GM/R_V^2$	9.82022
Precession constant ⁷	
$H = J_2 Ma^2/C$	3.2737634×10^{-3}
C (Polar moment)	$0.3307007 Ma^2$
B	$0.3296181 Ma^2$
A	$0.3296108 Ma^2$
Mean moment I	$0.3299765 Ma^2$
	$0.3307144 MR_{\oplus}^2$
Mean rotation rate: ω	$7.292115 \times 10^{-5} \text{ rad s}^{-1}$
$m_V = \omega^2 R_V^3/GM_{\oplus}$	$1/289.872$
$m = \omega^2 a^3/GM_{\oplus}$	$1/288.901$
Hydrostatic J_{2h}	0.0010722
Hydrostatic f_h	$1/299.66$
Fluid core radius(PREM)	3480 km
Inner core radius	1215 km
Mass of layers	
atmosphere	$5.1 \times 10^{18} \text{ kg}$
oceans	$1.4 \times 10^{21} \text{ kg}$
crust	$2.6 \times 10^{22} \text{ kg}$
mantle	$4.043 \times 10^{24} \text{ kg}$
outer core	$1.835 \times 10^{24} \text{ kg}$
inner core	$9.675 \times 10^{22} \text{ kg}$
Moments of inertia	
Mantle $I_m/M_{\oplus}a^2$	0.29215
Fluid core: $I_f/M_{\oplus}a^2$	0.03757

Table 2(cont). Geodetic and Geophysical data

Fluid core: $I_{f+ic}/M_{f+ic}a^2$	0.392
inner core: $I_{ic}/M_{\oplus}a^2$	2.35×10^{-4}
Hydrostatic $(C_f - A_f)/C_f$	1/393.10
Observed $(C_f - A_f)/C_f$	1/373.81
Hydrostatic $(C_{ic} - A_{ic})/C_{ic}$	1/416
Free core nutation period ⁴	429.8 d
Chandler wobble period ⁵	434.3 d
Surface area ⁶	
land	$1.48 \times 10^8 \text{ km}^2$
sea	$3.62 \times 10^8 \text{ km}^2$
total	$5.10 \times 10^8 \text{ km}^2$

Table 2: References: 1) Rapp [90]; 2) Geodetic Reference system [74]; 3) Souchay and Kinoshita [100] and Kinoshita (priv. comm.). 4) Herring *et al.* [49]. 5) Clark and Vicente [23] also find that the Chandler wobble Q is 179(74, 790). 6) Stacey [101]. 7) Williams [116]. Moments of inertia of each internal unit are based on the PREM model and were provided by E. Ivins.

Table 3a. Moon: Physical Data

GM ^a	4902.798 ± 0.005
M_{\oplus}/M ^b	81.300587 ± 0.000049
Mass	$7.349 \times 10^{22} \text{ kg}$
Radius R_V ^c	$1737.53 \pm 0.03 \text{ km}$
Density	3.3437
	$\pm 0.0016 \text{ gm cm}^{-3}$
Surface gravity	1.62 m s^{-2}
$\beta = (C - A)/B$ ^b	$6.31(72 \pm 15) \times 10^{-4}$
$\gamma = B - A/C$	$2.278(8 \pm 2) \times 10^{-4}$
Moment of inertia: C/MR^2	
^a	0.3935 ± 0.0011
^{b,d}	0.3940 ± 0.0019
Heat flow ^e	
Apollo 15	$3.1 \pm 0.6 \text{ mW m}^{-2}$
Apollo 17	$2.2 \pm 0.5 \text{ mW m}^{-2}$
Crustal thickness	
nearside ^f	$58 \pm 8 \text{ km}$
farside ^{c,g}	$\sim 80 - 90 \text{ km}$
Mean crustal density ^g	$2.97 \pm 0.07 \text{ gm cm}^{-3}$
k_2	0.0302 ± 0.0012
Tidal Q (see note ^h)	26.5 ± 1.0
Induced magnetic moment ^j	$4.23 \times 10^{22} \text{ G cm}^3$
Core radius constraints	
Source	Radius (km)

TABLE 3a. (continued).

Magnetometer moment ⁱ	435 ± 15
Seismic ^f	< 500
$I = 0.3933$	~ 350
LLR ^h	~ 400
Semimajor axis	384400km
	$60.27R_{\oplus}$
Orbit eccentricity	0.05490
Inclination	5.145°
Mean motion n	$2.6616995 \times 10^{-6} \text{ rad s}^{-1}$
Orbit period	27.321582 d
Nodal period	6798.38 d
Apsidal period	3231.50 d
Obliquity to orbit	6.67°
Mean Angular Diameter	31'05''2

Table 3b. Seismic velocity profiles

Depth km	Q_S km s^{-1}	Q_P km s^{-1}
-------------	-----------------------------	-----------------------------

Nakamura ^f		
0 – 1	0.29	0.51
1 – 15	2.82	4.90
15 – 30	3.59	6.25
30 – 58	3.84	6.68
58 – 270	4.49 ± 0.03	7.74 ± 0.12
270 – 500	4.25 ± 0.10	7.46 ± 0.25
500 – 1000	4.65 ± 0.16	8.26 ± 0.40
Goins <i>et al.</i> ^k		
0 – 20	2.96	5.10
20 – 60	3.90	6.80
60	4.57 ± 0.05	7.75 ± 0.15
400	4.37 ± 0.05	7.65 ± 0.15
480	4.20 ± 0.10	7.60 ± 0.60
1100	4.20 ± 0.10	7.60 ± 0.60

Seismic Q ^f

Depth km	Q_S km s^{-1}	Q_P km s^{-1}
-------------	-----------------------------	-----------------------------

0-60	~ 6000	~ 6000
60-270	4000+	$4000 - 7000+$
270-500	~ 1500	
500 – 1000	$< 100(?)$	

Table 3c. Lunar gravity field ^{a,b}

<i>nm</i>	$C_{nm} \times 10^9$	$S_{nm} \times 10^9$
20	-203805 ± 570	
22	22372 ± 110	
30	-8252 ± 600	
	$[-8610 \pm 230]$	
31	28618 ± 190	5871 ± 200
32	4891 ± 100	1646 ± 90
	$[4827 \pm 30]$	$[1682 \pm 11]$
33	1727 ± 35	-211 ± 34
	$[1710 \pm 100]$	$[-270 \pm 30]$
40	9235 ± 72	
41	-4032 ± 14	97 ± 15
42	1691 ± 73	1478 ± 61
43	94 ± 21	798 ± 22
44	127 ± 8	74 ± 6
50	-2552 ± 800	
60	15152 ± 1500	

Bracketed [] terms are from a 1994 LLR solution.

Table 3: Notes and references: a) New solution for lunar GM and gravity field ($R_e = 1738$ km) obtained by Konopliv *et al.* [61] using lunar orbiter and Apollo spacecraft Doppler data for which the realistic error is estimated to be 10 times formal σ (except for GM which is 4σ).

b) Lunar laser ranging (LLR) solution from Williams *et al.* [114] and Dickey *et al.* [32].
 c) Bills and Ferrari [9].
 d) Ferrari *et al.* [38] and Dickey *et al.* [32].
 e) Heiken [48].
 f) Crustal thickness beneath Apollo 12 and 14 sites from

Table 3d. Low order topography ^c

<i>nm</i>	$C_{nm} \times 10^6$	$S_{nm} \times 10^6$
10	-367.7 ± 44.6	
11	-1049.3 ± 30.3	-255.4 ± 23.6
20	-303.9 ± 49.5	
21	-193.4 ± 34.2	30.4 ± 24.9
22	7.4 ± 7.4	107.8 ± 9.4

Table 3e. Retroreflector coordinates ^b

Station	Radius meters	Longitude degrees	Latitude degrees
Apollo 11	1735474.22	23.472922	0.673390
Apollo 14	1736338.34	-17.478790	-3.644200
Apollo 15	1735477.76	3.628351	26.133285
Lunakhod 2	1734638.78	30.921980	25.832195

Nakamura [76, 77].

g) Farside thickness estimated from 2 km center of figure - center of mass offset [9].

h) Based on 1994 LLR solution [32]. The LLR Q signature is a $0.26'' \cos F$ amplitude figure libration which is 90° out of phase with the primary term. This effect could just as easily be due to lunar fluid core mantle friction with core radius $\sim 300 - 400$ km [38, 119, 32].

j) Russell *et al.* [92].

k) Goins *et al.* [44]. Sellers [96] obtains a seismic upper bound for R_c of 450 km.

Table 4a. Lunar orbit: Angle Arguments

$$\begin{aligned}
 D &= 297^\circ 51' 00.735'' + 1602961601.4603T - 6.93659T^2 + 0.006559T^3 - 0.00003184T^4 \\
 \ell &= 134^\circ 57' 48.184'' + 1717915922.8022T + 31.2344T^2 + 0.051612T^3 - 0.00024470T^4 \\
 \ell' &= 357^\circ 31' 44.793'' + 129596581.0474T - 0.5529T^2 + 0.000147T^3 \\
 F &= 93^\circ 16' 19.558'' + 1739527263.0983T - 13.3498T^2 - 0.001057T^3 + 0.00000417T^4 \\
 \Omega &= 125^\circ 02' 40.39816'' - 6962890.2656T + 6.9366T^2 + 0.007702T^3 - 0.00005939T^4 \\
 L &= 218^\circ 18' 59.956'' + 1732564372.8326T - 5.84479T^2 + 0.006568T^3 - 0.0000317T^4
 \end{aligned}$$

Table 4: Major periodic orbit perturbations due to the Sun are from Chapront-Touze *et al.* [21] model. Lunar arguments: L is the lunar mean longitude, ℓ is the mean anomaly, $F = L - \Omega$ (ascending node) and $D = L - L'$. Solar angles are mean longitude L' and mean anomaly ℓ' . The time T has units of Julian centuries from J2000(JD2451545.0).

Factors of T^q have units of arc seconds Cy^{-q} , except for the constant term.

Changing the lunar acceleration from the adopted value of $-25.900''\text{Cy}^{-2}$ by $+1.00''\text{Cy}^{-2}$, changes the T^2 coefficient of D and L by $+0.55042''T^2$, ℓ by $+0.55853''T^2$ and F by $+0.54828''T^2$.

Table 4b. Truncated Lunar Orbit Model

radius (km)	=	$385000 - 20905 \cos \ell - 3699 \cos(2D - \ell) - 2956 \cos 2D - 570 \cos 2\ell + 246 \cos(2D - 2\ell) - 205 \cos(2D - \ell') - 171 \cos(2D + \ell)$
longitude (")	=	$L + 22640 \sin \ell + 4586 \sin(2D - \ell) + 2370 \sin 2D + 769 \sin 2\ell - 666 \sin \ell' - 412 \sin 2F + 212 \sin(2D - 2\ell) + 205 \sin(2D - \ell - \ell') + 192 \sin(2D + \ell) + 165 \sin(2D - \ell) + 147 \sin(\ell - \ell') - 125 \sin D$
latitude (")	=	$18461 \sin F + 1010 \sin(F + l) + 1000 \sin(\ell - F) + 624 \sin(2D - F) + 200 \sin(2D - \ell + F) + 167 \sin(2D - \ell - F) + 117 \sin(4D + \ell)$

Table 5. Planetary Gravity Field

	Mercury	Venus	Earth	Mars
GM ($\text{km}^3 \text{s}^{-2}$)	22032.09	324858.63	398600.440	42828.3
σ_{GM}	± 0.91	± 0.04		± 0.1
GM_t			403503.235	
M_\odot/M_t	6023600	408523.61	328900.56	3098708
	± 250	± 0.15	± 0.02	± 9
R_e (km)	2440	6051.893	6378.137	3394.0
$J_2 (\times 10^{-6})$	60	4.458	1082.626523	1960.454
	± 20	± 0.026		± 0.18
C_{22}	10	0.539	1.5744	-54.73
	± 5	± 0.008	± 0.0004	± 0.02
S_{22}		-0.057	-0.9038	31.340
		± 0.010	± 0.0004	± 0.02
J_3		1.928	-2.112	31.45
		± 0.018	± 0.0020	± 0.51
J_4		2.381	-2.156	-18.89
		± 0.021	± 0.0030	± 0.72
	Jupiter	Saturn	Uranus	Neptune
GM ($\text{km}^3 \text{s}^{-2}$)	126,686,537	37,931,187	5,793,947	6,835,107
σ_{GM}	± 100	± 100	± 23	± 15
GM_t	126,712,767	37,940,554	5,794,560	6,836,534
	± 100	± 100	± 10	± 15
M_\odot/M_t	1047.3486	3497.898	22902.94	19412.240
	± 0.0008	± 0.018	± 0.04	± 0.057
R_e (km)	71398	60330	26200	25,225
$J_2 (\times 10^{-6})$	14736	16298	3343.43	3411
	± 1	± 10	± 0.32	± 10
J_4	-587	-915	-28.85	-35
	± 5	± 40	± 0.45	± 10
J_6	31	103		
	± 20	± 50		

Table 5: Planetary system GM_t , inverse system mass, planet GM , and selected gravity field coefficients and their corresponding reference radius R_e for Mercury [3], Venus [73, 60] (the quoted, realistic errors are 4× formal), Earth

(GEM T2) [71], Mars [5, 37], Jupiter [16], Saturn [17, 79], Uranus [40, 55] and Neptune [111].

$$GM_\odot = 1.3271243994 \times 10^{11} \text{ km}^3 \text{ s}^{-2}.$$

Table 6. Terrestrial Planets: Geophysical Data

	Mercury	Venus	Earth	Mars
Mean radius R_V (km)	2440 ± 1	$6051.8(4 \pm 1)$	$6371.0(1 \pm 2)$	$3389.9(2 \pm 4)$
Mass ($\times 10^{23}$ kg)	3.302	48.685	59.736	6.4185
Volume ($\times 10^{10}$ km 3)	6.085	92.843	108.321	16.318
Density (g cm $^{-3}$)	5.427	5.204	5.515	3.933(5 ± 4)
Flattening f			1/298.257	1/154.409
Semimajor axis			6378.136	3397 \pm 4
Sidereal rotation period	58.6462d	-243.0185d	23.93419hr	24.622962hr
Rotation rate ω ($\times 10^5$ s)	0.124001	-0.029924	7.292115	7.088218
Mean solar day (in days)	175.9421	116.7490	1.002738	1.0274907d
$mV = \omega^2 R_V^3/GM$	10×10^{-7}	61×10^{-9}	0.0034498	0.0045699
Polar gravity (m s $^{-2}$)			9.832186	3.758
Equatorial gravity (m s $^{-2}$)	3.701	8.870	9.780327	3.690
Moment of inertia: I/MR_o^2	0.33	0.33	0.3308	0.366
Core radius (km)	~ 1600	~ 3200	3485	~ 1700
Potential Love no. k_2		~ 0.25	0.299	~ 0.14
Grav. spectral factor: u ($\times 10^5$)		1.5	1.0	14
Topo. spectral factor: t ($\times 10^5$)		23	32	96
Figure offset ($R_{CF} - R_{CM}$) (km)		0.19 ± 01	0.80	2.50 ± 0.07
Offset (lat./long.)		$11^\circ/102^\circ$	$46^\circ/35^\circ$	$62^\circ/88^\circ$
Planetary Solar constant (W m 2)	9936.9	2613.9	1367.6	589.0
Mean Temperature (K)		735	270	210
Atmospheric Pressure (bar)		90	1.0	0.0056
Maximum angular diameter	11''0	60''2		17''9''
Visual magnitude V(1,0)	-0.42	-4.40	-3.86	-1.52
Geometric albedo	0.106	0.65	0.367	0.150
Obliquity to orbit (deg)	~ 0.1	177.3	23.45	25.19
Sidereal orbit period (yr)	0.2408445	0.6151826	0.9999786	1.88071105
Sidereal orbit period (day)	87.968435	224.695434	365.242190	686.92971
Mean daily motion: n (° d $^{-1}$)	4.0923771	1.6021687	0.9856474	0.5240711
Orbit velocity (km s $^{-1}$)	47.8725	35.0214	29.7859	24.1309
Escape velocity v_∞ (km s $^{-1}$)	4.435	10.361	11.186	5.027
Hill's sphere radius (R_p)	94.4	167.1	234.9	319.8
Magnetic moment (gauss R_p^{-3})			0.61	$< 1 \times 10^{-4}$

Table 6: Geodetic data for Mercury [46], Venus [73], Earth and Mars [10, 37]. Except for Venus [73], gravity and topographic field strength coefficients are from [11].

Venus topography: The topographic second harmonic (normalized) coefficients of Venus [73] are:

$$\overline{C}_{20}^T = -25 \times 10^{-6}; \overline{C}_{21}^T = 14 \times 10^{-6}; \overline{S}_{21}^T = -8 \times 10^{-6}; \\ \overline{C}_{22}^T = -20 \times 10^{-6}; \overline{S}_{22}^T = -5 \times 10^{-6}.$$

Of Mars [10] are:

$$\overline{C}_{20}^T = -1824 \pm 12 \times 10^{-6}; \overline{C}_{21}^T = 72 \pm 12 \times 10^{-6}; \overline{S}_{21}^T =$$

$$103 \pm 12 \times 10^{-6}; \overline{C}_{22}^T = -288 \pm 10 \times 10^{-6}; \overline{S}_{22}^T = -0.5 \times 10^{-6}$$

The derivation of Mars' mean moment of inertia assumes that Tharsis is the primary non-hydrostatic source and that the hydrostatic

$$J_{2h} = J_2 - (B - A)/2MR_e^2 = 0.001832.$$

Except for Earth, the values for mean moment I , potential Love number k_2 , core radius and mass are model calculations based on plausible structure [7].

Table 7. Giant Planets: Physical Data

	Jupiter	Saturn	Uranus	Neptune
Mass (10^{24} kg)	1898.6	568.46	86.832	102.43
Density (g cm^{-3})	1.326	0.6873	1.318	1.638
Equatorial radius (1 bar) a (km)	71492 ± 4	60268 ± 4	25559 ± 4	24766 ± 15
Polar radius b (km)	66854 ± 10	54364 ± 10	24973 ± 20	24342 ± 30
Volumetric mean radius: R_V (km)	69911 ± 6	58232 ± 6	25362 ± 12	24624 ± 21
flattening $f = (a - b)/a$	0.06487 ± 0.00015	0.09796 ± 0.00018	^A 0.02293 ± 0.0008	0.0171 ± 0.0014
Rotation period: T_{mag}	$9^{\text{h}}55^{\text{m}}27^{\text{s}}3$	$10^{\text{h}}39^{\text{m}}22^{\text{s}}4$	17.24 ± 0.01 h	16.11 ± 0.01 h
Rotation rate ω_{mag} (10^{-4} rad s $^{-1}$)	1.75853	1.63785	1.012	1.083
$m = \omega^2 a^3/GM$	0.089195	0.15481	0.02954	0.02609
Hydrostatic flattening f_h ^B	0.06509	0.09829	0.01987	0.01804
Inferred rotation period T_h (hr)	9.894 ± 0.02	10.61 ± 0.02	17.14 ± 0.9	16.7 ± 1.4
$k_s = 3J_2/m$	0.494	0.317	0.357	0.407
Moment of inertia: I/MR_o^2 ^C	0.254	0.210	0.225	
I/MR^2_o (upper bound) ^D	0.267	0.231	0.232	0.239
Rocky core mass (M_c/M_\oplus) ^C	0.0261	0.1027	0.0012	
Y factor (He/H ratio)	0.18 \pm 0.04	0.06 \pm 0.06	0.262 \pm 0.048	0.235 \pm 0.040
Equatorial gravity g_e (m s $^{-2}$)	23.12 ± 0.01	8.96 ± 0.01	8.69 ± 0.01	11.00 ± 0.05
Polar gravity g_p (m s $^{-2}$)	27.01 ± 0.01	12.14 ± 0.01	9.19 ± 0.02	11.41 ± 0.03
Geometric albedo	0.52	0.47	0.51	0.41
Visual magnitude $V(1,0)$	-9.40	-8.88	-7.19	-6.87
Visual magnitude (opposition)	-2.70	+0.67	+5.52	+7.84
Obliquity to orbit (deg)	3.12	26.73	97.86	29.56
Sidereal orbit period (yr)	11.856523	29.423519	83.747407	163.72321
Sidereal orbit period (day)	4330.595	10746.940	30588.740	59799.900
Mean daily motion n ($^{\circ}$ d $^{-1}$)	0.0831294	0.0334979	0.0117690	0.0060200
Mean orbit velocity (km s $^{-1}$)	13.0697	9.6624	5.4778	4.7490
Atmospheric temperature (1 bar) (K)	165 ± 5	134 ± 4	76 ± 2	72 ± 2
Heat flow/Mass ($\times 10^7$ erg g $^{-1}$ s $^{-1}$)	15	15	0.6 ± 0.6	2
Planetary solar constant (W m $^{-2}$)	50.5	15.04	3.71	1.47
Mag. dipole moment (gauss- R_p^3)	4.2	0.21	0.23	0.133
Dipole tilt/offset (deg/ R_p)	9.6/0.1	0.0/0.0	58.6/0.3	47/0.55
Escape velocity v (km s $^{-1}$)	59.5	35.5	21.3	23.5
$A_{\text{Roche}}(\text{ice})/R_p$	2.76	2.71	2.20	2.98
Hill's sphere radius h (in R_p)	740	1100	2700	4700

Table 7: Geodetic and temperature data (1 bar pressure level) for the giant planets obtained from Voyager radio occultation experiments for Jupiter [66], Saturn [67], Uranus [68] and Neptune [111, 69]. The magnetic field rotation periods (system III) and dipole moment for Jupiter, Saturn [25], Uranus and Neptune [78].

Notes:

A) The Uranian flattening determined from stellar occultations [6] is significantly smaller $f = 0.0019(7 \pm 1)$ at

1 μ bar than at the 1 bar level. The heat flow and Y factor are from Podolak *et al.* [89]. Geometric albedos and visual magnitudes are from Seidelmann[95].

B) The hydrostatic flattening is derived from (28), using the observed J_2 and the magnetic field rotation rate. The inferred mean rotation rate uses J_2 and the observed flattening (for Uranus, I adopt $f = 0.0019(7 \pm 1)$).

C) Upper bounds to the mean moment of inertia using (30) with $\delta_1 = 0$. D) Hubbard and Marley [52] solution.

Table 8. Planetary Mean Orbits

Planet	A AU $AU Cy^{-1}$	e Cy^{-1}	I deg "Cy $^{-1}$	Ω deg "Cy $^{-1}$	$\tilde{\omega}$ deg "Cy $^{-1}$	L deg "Cy $^{-1}$
Mercury	0.38709893 0.00000066	0.20563069 0.00002527	7.00487 -23.51	48.33167 -446.30	77.45645 573.57	252.25084 538101628.29
<i>mean orbit</i>	0.38709880 0.00002041	0.20563175 0.00002041	7.00499 -21.43	48.33089 -451.52	77.45612 571.91	252.25091 538101628.89
Venus	0.72333199 0.00000092	0.00677323 -0.00004938	3.39471 -2.86	76.68069 -996.89	131.53298 -108.80	181.97973 210664136.06
	0.72333201	0.00677177 -0.00004777	3.39447 -3.08	76.67992 -1000.85	131.56371 17.55	181.97980 21066136.43
Earth	1.00000011 -0.00000005	0.01671022 -0.00003804	0.00005 -46.94	-11.26064 -18228.25	102.94719 1198.28	100.46435 129597740.63
	1.00000083	0.016708617 -0.00004204	0.0 -46.60	0.0 -867.93	102.93735 1161.12	100.46645 129597742.28
Mars	1.52366231 -0.00007221	0.09341233 0.00011902	1.85061 -25.47	49.57854 -1020.19	336.04084 1560.78	355.45332 68905103.78
	1.52368946	0.09340062 0.00009048	1.84973 -29.33	49.55809 -1062.90	336.60234 1598.05	355.43327 68905077.49
Jupiter	5.20336301 0.00060737	0.04839266 -0.00012880	1.30530 -4.15	100.55615 1217.17	14.75385 839.93	34.40438 10925078.35
	5.20275842	0.04849485 0.00016322	1.30327 -7.16	100.46444 636.20	14.33131 777.88	34.35148 10925660.38
Saturn	9.53707032 -0.00301530	0.05415060 -0.00036762	2.48446 6.11	113.71504 -1591.05	92.43194 -1948.89	49.94432 4401052.95
	9.54282442	0.05550862 -0.00034664	2.48888 9.18	113.66552 -924.02	93.05678 2039.55	50.07747 4399609.86
Uranus	19.19126393 0.00152025	0.04716771 -0.00019150	0.76986 6.11	74.22988 -1591.05	170.96424 -1948.89	313.23218 1513052.95
	19.19205970	0.04629590 -0.00002729	0.77320 -6.07	74.00595 266.91	173.00516 321.56	314.05501 1542481.19
Neptune	30.06896348 -0.00125196	0.00858587 0.00002514	1.76917 -3.64	131.72169 -151.25	44.97135 -844.43	304.88003 786449.21
	30.06893043	0.00898809 0.00000603	1.76995 8.12	131.78406 -22.19	48.12369 105.07	304.34867 786550.32
Pluto	39.48168677 -0.00076912	0.24880766 0.00006465	17.14175 11.07	110.30347 -37.33	224.06676 -132.25	238.92881 522747.90

Table 8: This table contains two distinct mean orbit solutions referenced to the J2000 epoch. First, a 250 yr. least squares fit (first two rows for each planet) of the DE 200 planetary ephemeris [103] to a Keplerian orbit where each element is allowed to vary linearly with time. This solution fits the terrestrial planet orbits to $\sim 25''$ or better, but achieves only $\sim 600''$ for Saturn. The second solution (the third and fourth rows for each planet) is a mean element solution (from

table 15.6 in [95]), except that the semimajor axis is the average value defined by eq(37). The fit for this case over the same 250 yr. is worse (M. Standish, priv. comm.) for the giant planets because of pairwise near commensurabilities in the mean motions of Jupiter-Saturn ($S_1 = (2L_5 - 5L_6)$ with 883 yr. period) and Uranus-Neptune ($S_2 = (L_7 - 2L_8)$ with 4233 yr. period). However, the mean orbit should be more stable over longer periods.

Table 9. North Pole of Rotation (α_0 , δ_0 and Prime Meridian) of Planets and Sun

	α_0 deg	δ_0 deg	W (prime meridian) deg	reference feature
Sun	286.13	63.87	$84.10 + 14.1844000d$	
Mercury	$281.01 - 0.003T$	$61.45 - 0.005T$	$329.71 + 6.1385025d$	Hun Kai(20.00° W)
Venus ^A	272.76	67.16	$160.20 - 1.481545d$	Ariadne(central peak)
Earth	$0.00 - 0.641T$	$90.00 - 0.557T$	$190.16 + 306.9856235d$	Greenwich,England
Mars	$317.681 - 0.108T$	$52.886 - 0.061T$	$176.868 + 350.8919830d$	crater Airy-0
Jupiter	$268.05 - 0.009T$	$64.49 + 0.003T$	$284.95 + 870.53600000d$	magnetic field
Saturn ^B	$40.5954 - 0.0577T$	$83.5380 - 0.0066T$	$38.90 + 810.7939024d$	magnetic field
Uranus ^C	257.43	-15.10	$203.81 - 501.1600928d$	magnetic field
Neptune ^D	$299.36 + 0.70 \sin N$	$43.46 - 0.51 \cos N$	$253.18 + 536.3128492d - 0.48 \sin N$	
Pluto	313.02	9.09	$236.77 - 56.3623195d$	sub-Charon ^E

Table 9: Reference date is 2000 Jan 1.5 (JD 2451545.0). The time interval T (in Julian centuries) and d (days) from the standard epoch. The prime meridian W is measured from the ascending node of the planet equator on the J2000 earth equator to a reference point on the surface. Venus, Uranus and Pluto rotate in a retrograde sense.

A) The Magellan values [28] for α_0 , δ_0 and W for Venus are:

$$\alpha_0 = 272^\circ 76 \pm 0.02; \quad \delta_0 = 67^\circ 16 \pm 0.01; \\ W = 160^\circ 20 - 19^\circ 4813688d.$$

B) Saturn's pole is based on French *et al.* [42] which include the 1989 occultation of 28 Sgr. They claim detection of Saturn's pole precession rate.

C) Improved Uranian pole (B1950 epoch) position is [40]:
 $\alpha_0 = 256^\circ 5969 \pm 0.0034,$
 $\delta_0 = -15^\circ 1117 \pm 0.0033 .$

D) Neptune angle $N = 359^\circ 28 + 549^\circ 308T$.

E) The sub-Charon meridian on Pluto is fixed since Pluto rotates synchronously with Charon's orbit.

Invariable plane: The invariable plane coordinates are (J2000) [85]:

$$\alpha_0 = 273^\circ 8657; \quad \delta_0 = 66^\circ 9723.$$

This table is an updated version of the 1991 IAU [29] recommended values and also appears in [95].

Table 10. Pluto Charon System

GM_{sys}^1	$947 \pm 13 \text{ km}^3 \text{ s}^{-2}$
M_{sys}	$1.42 \pm 0.02 \times 10^{22} \text{ kg}$
Mass ratio (M_C/M_P) ¹ ²	0.12 0.1543 ± 0.0028
Mass of Pluto ¹ ²	$1.27 \pm 0.02 \times 10^{22} \text{ kg}$ $1.231 \pm 0.01 \times 10^{22} \text{ kg}$
Mass of Charon ¹ ²	$1.5 \times 10^{21} \text{ kg}$ $1.90 \pm 0.04 \times 10^{21} \text{ kg}$
Semi-major axis a ¹ ²	$19405 \pm 86 \text{ km}$ $19481 \pm 49 \text{ km}$
Eccentricity ³ e	$0.000(20 \pm 21)$
Inclination to mean equator & equinox ¹	$96.56 \pm 0.26^\circ$
Radius R_P ^{1,3} ⁴	$1137 \pm 8 \text{ km}$ $1206 \pm 11 \text{ km}$
Radius R_C	$586 \pm 13 \text{ km}$
Density of Pluto ($R = 1137 \pm 8 \text{ km}$) ¹ ($R = 1206 \pm 11 \text{ km}$) ¹ ($R = 1137 \pm 8 \text{ km}$) ² ($R = 1206 \pm 11 \text{ km}$) ²	2.06 g cm^{-3} 1.73 g cm^{-3} 2.00 g cm^{-3} 1.67 g cm^{-3}
Density of Charon ¹	1.8 g cm^{-3}
Density of Charon ²	2.24 g cm^{-3}
Orbital Period	$6.3872(30 \pm 21) \text{ d}$
Pluto's Albedo (blue & var.)	$0.43 - 0.60$
Charon's albedo	0.375 ± 0.08
Surface gravity	
Pluto ($R=1137 \text{ km}$) ¹	65.5 cm s^{-2}
Charon ¹	21.3 cm s^{-2}
Hill's Sphere (Charon) ¹	5800 km
Escape velocity (Charon) ¹	0.58 km s^{-1}
Planetary orbit period	248.0208 yr
Planetary orbit velocity	4.749 km s^{-1}

Table 10: 1) The discovery of a coordinate distortion in the HST camera reduces the mass ratio q from 0.0873 ± 0.0147 [83] to 0.12 [Null, priv. comm.], which is still low relative to q from low ground-based imaging [122]. Solution for semimajor axis and q determined from HST observations of the barycentric wobble of Pluto relative to a background star observed for 3.2 d [83].

2) Solution based on 6 nights of CCD imaging at Mauna Kea [].

3) The radii and period derive from mutual event data [15].

4) The presence of an atmosphere on Pluto introduces uncertainty into its radius. Models indicate that R_P is either $1206 \pm 6 \text{ km}$ (thermal gradient model) or $\leq 1187 \text{ km}$ (haze model) [34]. 5) Young and Binzel [123].

Table 11. Satellite Tidal Acceleration

Satellite	dn/dt	Notes
Moon		
Orbit		
(Optical ¹ astronomy) (LLR) ²	$-26.0 \pm 2.0 \text{ "Cy}^{-2}$	total
	$-22.24 \pm 0.6 \text{ "Cy}^{-2}$	$1/2 \text{ d \& l.p.}$
	$-4.04 \pm 0.4 \text{ "Cy}^{-2}$	1 d
	$+0.40 \text{ "Cy}^{-2}$	lunar tide
	$-25.88 \pm 0.5 \text{ "Cy}^{-2}$	total
Tidal gravity field (SLR) ³	$-22.10 \pm 0.4 \text{ "Cy}^{-2}$	$1/2 \text{ d}$
	-3.95 "Cy^{-2}	1 d
	$+0.18 \text{ "Cy}^{-2}$	l.p.
	$-25.8 \pm 0.4 \text{ "Cy}^{-2}$	total
Ocean tide height (GEOSAT) ⁴	$-25.0 \pm 1.8 \text{ "Cy}^{-2}$	total
Phobos ⁵	$24.74 \pm 0.35 \text{ " Cy}^{-2}$	$1/2 \text{ d}$
Io ⁶	$-29 \pm 14 \text{ " Cy}^{-2}$	$1/2 \text{ d}$

Table 11: 1) Morrison and Ward [75].

2) Lunar laser ranging (LLR) result [115] [32]. Separation of diurnal and semidiurnal bands is obtained from 18.6 yr modulation [113];

3) Result from satellite laser ranging to LAGEOS, STAR-LETTTE, etc [22] inferred from the observed tidal gravity field.

4) Altimeter result [22] [19] of the ocean tide, with estimated 7% uncertainty. Both the SLR and Geosat results have been augmented by a factor of $(1 + M/M_\oplus)(1 + 2(n_\oplus/n)^2)$ due to a deficient dynamical model which ignored a barycentric correction [113] and the solar contribution to mean motion (see eq(36)). The inferred solid body Q for earth is $\sim 340(100(\text{min}), \infty(\text{max}))$.

5) Sinclair's solution [97] is typical of several independent analyses of both ground-based and spacecraft data. The tidal acceleration due to solid tides is $dn/dt = k_2/Q \times (15260 \pm 150) \text{ "Cy}^{-2}$ [120], from which we can deduce Mars' $Q = 86 \pm 2$ for $k_2 = 0.14$. If Mars' k_2 is larger, Q is also larger.

6) Io's acceleration is from analysis of 3 Cy of Galilean satellite observations [65] and the above LLR value for earth moon's dn/dt . An equivalent form is:

$$dn_{\text{Io}}/dt = n_{\text{Io}} \times (-1.09 \pm 0.50) \times 10^{-11} \text{ yr}^{-1}.$$

Lieske [65] also finds

$$d/dt(n_{\text{Io}} - n_{\text{Europa}}) = n_{\text{Io}} \times (+0.08 \pm 0.42) \times 10^{-11} \text{ yr}^{-1}.$$

Table 12. Planetary Satellites: Physical Properties

Satellite	Radius (km)	Mass 10^{20} kg	Density gm cm $^{-3}$	Geom. albedo	V(1,0)
Earth	6378	59742	5.515	0.367	-3.86
Moon	1737.53 ± 0.03	734.9	3.34	0.12	+0.21
Mars	3394	641.9	3.933	0.150	-1.52
M1 Phobos ^{1,2}	$13.1 \times 11.1 \times 9.3 (\pm 0.1)$	$1.08 (\pm 0.01) \times 10^{-4}$	1.90 ± 0.08	0.06	+11.8
M2 Deimos ²	$(7.8 \times 6.0 \times 5.1) (\pm 0.2)$	$1.80 (\pm 0.15) \times 10^{-5}$	1.76 ± 0.30	0.07	+12.89
Jupiter	71492	1.8988×10^7	1.326	0.52	-9.40
JXVI Metis	20 ± 10			0.05	+10.8
JXV Adrastea	10 ± 10			0.05	+12.4
JV Almethaea	$(131 \times 73 \times 67) (\pm 3)$			0.05	+7.4
JXIV Thebe	50 ± 10			0.05	+9.0
JI Io ³	1821.3 ± 0.2	893.3 ± 1.5	3.530 ± 0.006	0.61	
JII Europa	1565 ± 8	479.7 ± 1.5	2.99 ± 0.05	0.64	
JIII Ganymede	2634 ± 10	1482 ± 1	1.94 ± 0.02	0.42	
JIV Callisto	2403 ± 5	1076 ± 1	1.851 ± 0.004	0.20	
JXIII Leda	5				+13.5
JVI Himalia	85 ± 10				+8.14
JX Lysithea	12				+11.7
JXVI Elara	40 ± 10				+10.07
JXII Ananke	10				+12.2
JXI Carme	15				+11.3
JVIII Pasiphae	18				+10.33
JIX Sinope	14				+11.6
Saturn	60268	$5.6850E6$	0.687	0.47	-8.88
XVIII Pan	10			0.5	
SXV Atlas	$(18.5 \times 17.2 \times 13.5) (\pm 4)$			0.9	+8.4
XVI Prometheus ⁴	$74 \times 50 \times 34 (\pm 3)$	$0.001(4)^{+8}_{-7}$	0.27 ± 0.16	0.6	+6.4
SXVII Pandora	$(55 \times 44 \times 31) (\pm 2)$	$0.001(3)^{+8}_{-7}$	0.42 ± 0.28	0.9	+6.4
SX Janus ⁵	$(99.3 \times 95.6 \times 75.6) (\pm 3)$	0.0198 ± 0.0012	0.65 ± 0.08	0.8	+4.4
SXI Epimetheus	$(69 \times 55 \times 55) (\pm 3)$	0.0055 ± 0.0003	0.63 ± 0.11	0.8	+5.4
SI Mimas ⁶	198.8 ± 0.6	0.375 ± 0.009	1.14 ± 0.02	0.5	+3.3
SII Enceladus ⁷	249.1 ± 0.3	0.73 ± 0.36	1.12 ± 0.55	1.0	+2.1
SIII Tethys ⁸	529.9 ± 1.5	6.22 ± 0.13	1.00 ± 0.02	0.9	+0.6
SXIV Calypso(T-)	$15 \times 8 \times 8 (\pm 4)$			0.6	+9.1
SXIII Telesto(T+)	$15(2.5) \times 12.5(5) \times 7.5(2.5)$			0.5	+8.9
SIV Dione ⁸	560 ± 5	10.52 ± 0.33	1.44 ± 0.06	0.7	+0.8
SXII Helene(T+)	16 ± 5			0.7	+8.4
Saturn	60268	$5.6850E6$	0.687	0.47	-8.88
SV Rhea	764 ± 4	23.1 ± 0.6	1.24 ± 0.04	0.7	+0.1
SVI Titan	2575 ± 2	1345.5 ± 0.2	1.881 ± 0.005	0.21	-1.28
SVII Hyperion ⁹	$(185 \times 140 \times 113) (\pm 10)$			$0.19 - 0.25$	+4.6
SVIII Iapetus	718 ± 8	15.9 ± 1.5	1.02 ± 0.10	$0.05 - 0.5$	+1.5
SIX Phoebe	$(115 \times 110 \times 105) (\pm 10)$			0.06	+6.89

Table 12(cont). Planetary Satellites: Physical Properties

Satellite	Radius (km)	Mass 10^{20} kg	Density gm cm^{-3}	Geom. albedo	$V(1,0)$
Uranus ¹⁰	25559	$8.6625E5$	1.318	0.51	-7.19
VI Cordelia	13 ± 2			0.07	+11.4
VII Ophelia	16 ± 2			0.07	+11.1
VIII Bianca	22 ± 3			0.07	+10.3
IX Cressida	33 ± 4			0.07	+9.5
X Desdemona	29 ± 3			0.07	+9.8
XI Juliet	42 ± 5			0.07	+8.8
XII Portia	55 ± 6			0.07	+8.3
XIII Rosalind	29 ± 4			0.07	+9.8
XIV Belinda	34 ± 4			0.07	+9.4
XV Puck	77 ± 3			0.07	+7.5
UV Miranda	$240(0.6) \times 234.2(0.9) \times 232.9(1.2)$	0.659 ± 0.075	1.20 ± 0.14	0.27	+3.6
UI Ariel	$581.1(0.9) \times 577.9(0.6) \times 577.7(1.0)$	13.53 ± 1.20	1.67 ± 0.15	0.34	+1.45
UII Umbriel	584.7 ± 2.8	11.72 ± 1.35	1.40 ± 0.16	0.18	+2.10
UIII Titania	788.9 ± 1.8	35.27 ± 0.90	1.71 ± 0.05	0.27	+1.02
UIV Oberon	761.4 ± 2.6	30.14 ± 0.75	1.63 ± 0.05	0.24	+1.23
Neptune	24764	$1.0278E6$	1.638	0.41	-6.87
NIII Naiad	29			0.06	+10.0
NIV Thalassa	40			0.06	+9.1
NV Despina	74 ± 10			0.06	+7.9
NVI Galatea	79 ± 12			0.06	+7.6
NVII Larissa	$104 \times 89(\pm 7)$			0.06	+7.3
NVIII Proteus	$218 \times 208 \times 201$			0.06	+5.6
NI Triton	1352.6 ± 2.4	214.7 ± 0.7	2.054 ± 0.032	0.7	-1.24
NII Nereid	170 ± 2.5			0.2	+4.0

Table 12: Satellite radii are primarily from Davies *et al.* [29]. For synchronously locked rotation, the satellite figure's long axis points toward the planet while the short axis is normal to the orbit. Geometric and visual magnitude $V(1, 0)$ (equivalent magnitude at 1 AU and zero phase angle) are from [95]; $V_{\odot}(1, 0) = -26.8$. Satellite masses are from a variety of sources: Galilean satellites [16]; Saturnian large satellites [17]; Uranian large satellites [55]; Triton: mass [111] and radius [27].

Notes:

1) Duxbury [33, 8] has obtained an $n = j = 8$ harmonic expansion of Phobos' topography and obtains a mean radius of 11.04 ± 0.16 and mean volume of $5680 \pm 250 \text{ km}^3$ based on a model derived from over 300 normal points. The Phobos mission resulted in a much improved mass for Phobos [4].

2) Thomas (priv. comm.).

3) Gaskell *et al.* [43] find from analysis of 328 surface normal points that the figure axes are $(1830.0 \text{ km} \times 1818.7 \text{ km} \times 1815.3 \text{ km})(\pm 0.2 \text{ km})$. The observed $(b - c)/(a - c) = 0.23 \pm 0.02$, close to the hydrostatic value of $1/4$, while $f_1 = 0.00803 \pm 0.00011$ is consistent with $I/MR^2 = 0.382 \pm 0.003$.

4). The masses of Prometheus and Pandora [91] should be viewed with caution since they are estimated from ampli-

tudes of Lindblad resonances they excite in Saturn's rings.

5) Janus' radii are from [121]. Thomas [107] independently finds radii $97 \times 95 \times 77(\pm 4)$ for Janus. The coorbital satellite masses include new IR observations [81] and are firm. Rosen *et al.* [91] find $1.31^{(+1.7)}_{(-0.3)} \times 10^{18} \text{ kg}$ for Janus and $0.33^{(+0.11)}_{(-0.06)} \times 10^{18} \text{ kg}$ for Epimetheus from density wave models.

6) Dermott and Thomas find that the observed $(b - c)/(a - c) = 0.27 \pm 0.04$ for Mimas [30] and $(b - c)/(a - c) = 0.24 \pm 0.15$ for Tethys [108], and deduce that Mimas $I/MR^2 = 0.35 \pm 0.01$, based on a second order hydrostatic model.

7) Dermott and Thomas (priv. comm.) estimate Enceladus' mass = $0.66 \pm 0.01 \times 10^{23} \text{ gm}$ and density = $1.01 \pm 0.02 \text{ gm cm}^{-3}$ from its shape.

8) Harper and Taylor [47].

9) Klavetter [59] has verified that Hyperion rotates chaotically from analysis of 10 weeks of photometer data. Furthermore, he finds that the moment ratios are $A/C = 0.54 \pm 0.05$ and $B/C = 0.86 \pm 0.16$ from a fit of the light curve to a dynamic model of the tumbling.

10) The radii of the small Uranian satellites are from Thomas, Weitz and Veverka [106]. Masses of major satellites are from Jacobson *et al.* [55].

Table 13. Planetary Satellites: Orbital Data

Planet	Satellite	<i>a</i> (10 ³ km)	Orbital period days	Rot. period days	<i>e</i>	<i>I</i> deg
Earth	Moon	384.40	27.321661	S	0.054900	5.15
Mars	I Phobos	9.3772	0.318910	S	0.0151	1.082
	II Deimos	23.4632	1.262441	S	0.00033	1.791
Jupiter	XVI Metis ¹	127.96	0.294780	S	< 0.004	~ 0
	XV Adrastea ¹	128.98	0.29826	S	~ 0	~ 0
	V Almathea ¹	181.3	0.498179	S	0.003	0.40
	XIV Thebe	221.90	0.6745		0.015	0.8
	I Io	421.6	1.769138	S	0.041	0.040
	II Europa	670.9	3.551810	S	0.0101	0.470
	III Ganymede	1,070	7.154553	S	0.0015	0.195
	IV Callisto	1,883	16.689018	S	0.007	0.281
	XIII Leda	11,094	238.72		0.148	*27
	VI Himalia	11,480	250.5662	0.4	0.163	*175.3
	X Lysithea	11,720	259.22		0.107	*29
	VII Elara	11,737	259.6528	0.5	0.207	*28
	XII Ananka	21,200	631R		0.169	*147
	XI Carme	22,600	692R		0.207	*163
	VIII Pasiphae	23,500	735R		0.378	*148
	IX Sinope	23,700	758R		0.275	*153
Saturn	XVIII Pan	133.583	0.5750			
	XV Atlas ²	137.64	0.6019		~ 0	~ 0
	XVI Prometheus ²	139.35	0.612986		0.0024	0.0
	XVII Pandora ²	141.70	0.628804		0.0042	0.0
	XI Epimetheus	151.422	0.694590	S	0.009	0.34
	X Janus	151.472	0.694590	S	0.007	0.14
	I Mimas	185.52	0.9424218	S	0.0202	1.53
	II Enceladus	238.02	1.370218	S	0.0045	0.02
	III Tethys	294.66	1.887802	S	0.0000	1.09
	XIV Calypso(T-)	294.66	1.887802		~ 0	~ 0
	XIII Telesto(T+)	294.66	1.887802		~ 0	~ 0
	IV Dione	377.40	2.736915	S	0.0022	0.02
	XII Helene(T+)	377.40	2.736915		0.005	0.2
	V Rhea	527.04	4.517500	S	0.001	0.35
	VI Titan	1221.85	15.945421		0.0292	0.33
	VII Hyperion	1481.1	21.276609	C	0.1042	0.43
	VIII Iapetus	3561.3	79.330183	S	0.0283	7.52
	IX Phoebe	12952	550.48R	0.4	0.163	*175.3
Uranus¹	VI Cordelia	49.752	0.335033		0.000	0.1
	VII Ophelia	53.764	0.376409		0.010	0.1
	VIII Bianca	59.165	0.434577		0.001	0.2
	IX Cressida	61.777	0.463570		0.000	0.0
	X Desdemona	62.659	0.473651		0.000	0.2
	XI Juliet	64.358	0.493066		0.001	0.1
	XII Portia	66.097	0.513196		0.000	0.1

Table 13(cont). Planetary Satellites: Orbital Data

Planet	Satellite	a 10^3 km	Orbital period days	Rot. period days	e	I deg
Neptune ²	XIII Rosalind	69.927	0.558459		0.000	0.3
	XIV Belinda	75.255	0.623525		0.000	0.0
	XV Puck	86.004	0.761832		0.000	0.3
	V Miranda	129.8	1.413	S	0.0027	4.22
	I Ariel	191.2	2.520	S	0.0034	0.31
	II Umbriel	266.0	4.144	S	0.0050	0.36
	III Titania	435.8	8.706	S	0.0022	0.10
	IV Oberon	582.6	13.463	S	0.0008	0.10
	III Naiad	48.227	0.294396		0.000	4.74
	IV Thalassa	50.075	0.311485		0.000	0.21
	V Despina	52.526	0.334655		0.000	0.07
	VI Galatea	61.953	0.428745		0.000	0.05
	VII Larissa	73.548	0.554654		0.000	0.20
	VIII Proteus	117.647	1.122315		0.000	0.55
	I Triton	354.76	5.876854R	S		156.834
	II Nereid	5513.4	360.13619		0.7512	*7.23
Pluto	I Charon	19.405	6.38723		0	0

Table 13: Abbreviations: R=retrograde orbit; T=: Trojan-like satellite which leads(+) or trails(−) by $\sim 60^\circ$ in longitude the primary satellite with same semimajor axis; (*) The local invariable reference plane (see equation 68) of these distant satellites is controlled by Sun rather than plane-

tary oblateness; S=synchronous rotation; C=chaotic rotation; References: From [95], with additional data for Saturn's F ring satellites [104], Jupiter's small satellites [105], the Uranian [84] and Neptune [86, 53] systems.

Table 14. Planetary Rings

Feature	Distance ^b km	r/R_e	Optical depth	Albedo	σ g cm^{-2}	e
Jupiter	71492	1.000				
Halo	> 100000	1.25 – 1.71	3×10^{-6}			
Main	> 122000	1.71 – 1.81	5×10^{-6}	[0.015]	$> 5 \times 10^{-6}$	
Gossamer	> 129000	1.8 – 3	1×10^{-7}			
Saturn	60268	1.000				
D ring	> 66900	> 1.11				
C inner edge	74658	1.239	0.05 – 0.35	0.12 – 0.30	0.4 → 5	
Titan ringlet	77871	1.292			17	0.00026
Maxwell ringlet	87491	1.452			17	0.00034
B inner edge	91975	1.526	0.4 – 2.5	0.4 – 0.6	20 – 100	
B outer edge ^c	117507	1.950				
Cassini division			0.05 – 0.15	0.2 – 0.4	5 – 20	
A inner edge	122340	2.030	0.4 – 1.0	0.4 → 0.6	30 – 40	
Encke gap ^b	133589	2.216				
A outer edge ^d	136775	2.269				
F-ring center	140374	2.329	0.1	0.6		0.0026

TABLE 14. (continued).

Feature	Distance ^b km	r/R_e	Optical depth	Albedo	σ g cm^{-2}	e
G-ring center	170000	2.82	1×10^{-6}			
E inner edge	~ 180000	3	1.5×10^{-5}			
E outer edge	~ 480000	8				
				Albedo $\times 10^{-3}$	Width km	e
Uranus ^c	25559	1.000				
6	41837	1.637	~ 0.3	~ 15	~ 1.5	0.0010
5	42235	1.652	~ 0.5	~ 15	~ 2	0.0019
4	42571	1.666	~ 0.3	~ 15	~ 2.5	0.0010
α	44718	1.750	~ 0.4	~ 15	$4 \rightarrow 10$	0.0008
β	45661	1.786	~ 0.3	~ 15	$5 \rightarrow 11$	0.0004
η	47176	1.834	≤ 0.4	~ 15	1.6	
γ	47626	1.863	≥ 1.5	~ 15	$1 \rightarrow 4$	0.0001
δ	48303	1.900	~ 0.5	~ 15	$3 \rightarrow 7$	
λ	50024	1.957	~ 0.1	~ 15	~ 2	
ϵ	51149	2.006	$0.5 \rightarrow 2.3$	18 ± 1	$20 \rightarrow 96$	0.0079
Neptune	24766	1.000				
Galle	~ 41900	1.692	$\sim 1 \times 10^{-4}$	[15]	~ 1700	
Leverrier	53200	2.148	0.01	[15]	~ 100	
1989N4R	~ 53200	2.148	$\sim 1 \times 10^{-4}$	[15]	~ 4000	
Adams(arcs)	62932	2.477	$0.01 - 0.1$	[15]	~ 15	

Table 14: See Nicholson and Dones [80] and for a review of ring properties. Bracketed [] albedos are adopted. Horn *et al.* [54] find from density wave analysis that the A ring mean surface desity is $\sigma = 45 \pm 11 \text{ gm cm}^{-2}$ for $a = 2.0 - 2.21R$, and $\sigma = 29 \pm 7 \text{ gm cm}^{-2}$ for $a = 2.22 - 2.27R$, with mass(A-ring)= $5.2 \times 10^{21} \text{ gm}$.

a) See Esposito *et al.* [36] for a more complete list of

Saturn's ring features.

b) Encke gap width=322 km.

c) Sharp B ring edge controlled by 2:1 Lindblad resonance with Janus.

d) Sharp A ring edge due to 7:6 Janus' resonance.

e) French *et al.* [41].

Table 15. Prominent Minor Planets or Asteroids

No.	Name	Dia. km	Tax	a AU	e	I deg	Ω deg	ω deg	M deg	Period year	rotation hrs
1	Ceres	933	G?	2.769	0.0780	10.61	80.0	71.2	287.3	4.607	9.075
2	Pallas	525		2.770	0.2347	34.81	172.6	309.8	273.8	4.611	7.811
4	Vesta	510	V	2.361	0.0906	7.14	103.4	150.1	43.3	3.629	5.342
10	Hygiea	429	C	3.138	0.1201	3.84	283.0	316.1	33.0	5.656	27.659
511	Davida	337	C	3.174	0.1784	15.94	107.3	339.0	244.5	5.656	5.130
704	Interamnia	333	F	3.064	0.1475	17.30	280.4	92.2	276.8	5.364	8.727
52	Europa	312	C	3.101	0.1002	7.44	128.6	337.0	92.6	5.460	5.631
15	Eunomia	272	S	2.644	0.1849	11.76	292.9	97.5	327.9	4.299	6.083
87	Sylvia	271	PC	3.490	0.0820	10.87	73.1	273.3	248.8	6.519	5.183
3	Juno	267	S	2.668	0.0258	13.00	169.9	246.7	115.4	4.359	7.210
16	Psyche	264	M	2.923	0.1335	3.09	149.9	227.5	318.7	4.999	4.196
31	Euphrosyne	248	C	3.146	0.2290	26.34	30.7	63.1	341.0	5.581	5.531

Table 15. (cont) Prominent Minor Planets or Asteroids

No.	Name	Dia. km	Tax	<i>a</i> AU	<i>e</i>	<i>I</i> deg	Ω deg	ω deg	<i>M</i> deg	Period year	Rotation hrs
65	Cybele	240	C	3.437	0.1044	3.55	155.4	109.8	20.1	6.372	4.041
107	Camilla	237	C	3.484	0.0842	9.93	173.5	296.0	139.7	6.503	4.840
624	Hektor	233	D	5.181	0.0246	18.23	342.1	178.0	2.9	11.794	6.921
88	Thisbe	232	C	2.767	0.1638	5.22	276.3	35.3	259.0	4.603	6.042
451	Patientia	230	C	3.062	0.0709	15.24	89.0	343.2	269.4	5.358	9.727
324	Bamberga	228	C	2.681	0.3409	11.14	327.8	43.4	189.6	4.390	29.43
48	Doris	225	C	3.110	0.0693	6.54	183.4	262.8	278.8	5.485	11.89
532	Herculina	225	S	2.771	0.1764	16.36	107.4	75.1	199.4	4.613	9.405
29	Amphitrite	219	S	2.555	0.0717	6.10	355.9	62.8	197.9	4.084	5.390
423	Diotima	217	C	3.067	0.0365	11.25	69.2	215.6	223.9	5.371	4.622
121	Hermione	217	C	3.438	0.1428	7.56	74.1	287.5	4.3	6.376	8.97
375	Ursula	216	C	3.126	0.1037	15.93	336.1	347.9	163.0	5.528	16.83
13	Egeria	215	G	2.576	0.0863	16.52	42.8	81.1	132.8	4.136	7.045
45	Eugenia	214	C	2.722	0.0821	6.60	147.4	86.0	188.9	4.490	5.699
94	Aurora	212	C	3.164	0.0814	8.01	2.5	51.8	223.8	5.628	7.22
7	Iris	203	S	2.386	0.2296	5.51	259.3	144.8	132.3	3.685	7.139
702	Alauda	202	C	3.195	0.0286	20.57	289.6	3.6	335.5	5.710	8.36
19	Fortuna	200	C	2.442	0.1580	1.57	210.9	182.0	287.9	3.817	7.445
24	Themis	200	C	3.126	0.1351	0.76	35.6	110.5	229.9	5.528	8.374
2060	Chiron			13.716	0.3816	6.93	208.6	339.0	315.0	50.801	5.918
130	Elektra	189	G	3.113	0.2182	22.88	145.3	234.7	177.2	5.492	5.225
22	Kalliope	187	M	2.912	0.0978	13.70	65.8	355.6	212.6	4.969	4.147
747	Winchester	178	C	2.995	0.3433	18.18	129.6	276.1	354.5	5.183	9.40
153	Hilda	175	C	3.975	0.1418	7.84	227.8	42.6	269.5	7.925	*8.11
334	Chicago	170	C	3.875	0.0407	4.66	130.1	136.5	300.6	7.627	9.19
51	Nemausa	153	G	2.366	0.0656	9.96	175.6	2.4	50.8	3.640	7.785
617	Patroclus	149	P	5.230	0.1396	22.04	43.8	306.8	32.1	11.961	* > 40.
420	Bertholda	146	P	3.416	0.0475	6.70	243.9	206.3	158.8	6.314	11.04
69	Hesperia	143	M	2.979	0.1673	8.55	185.2	285.8	34.6	5.142	5.655
8	Flora	141	S	2.201	0.1564	5.89	110.5	284.8	176.3	3.266	12.790
216	Kleopatra	140	M	2.795	0.2495	13.11	215.2	179.4	312.4	4.674	5.385
279	Thule	135	D	4.271	0.0119	2.34	73.2	76.7	17.8	8.825	7.44
419	Aurelia	133	F	2.595	0.2562	3.95	229.3	43.1	147.7	4.179	16.709
221	Eos	110	K	3.012	0.0973	10.87	141.6	191.9	20.9	5.229	10.436
233	Asterope	108	T	2.661	0.0996	7.68	221.8	125.3	72.1	4.342	19.70
181	Eucharis	107	K	3.137	0.2032	18.69	143.5	313.2	98.8	5.555	* > 7.
114	Kassandra	103	T	2.675	0.1398	4.95	163.8	352.0	151.4	4.376	10.758
773	Irmintraud	99	D	2.858	0.0805	16.68	322.1	331.6	21.3	4.831	
25	Phocaea	78	S	2.400	0.2557	21.58	213.7	90.5	189.5	3.719	9.945
44	Nysa	73	E	2.424	0.1497	3.71	131.0	342.0	142.7	3.773	6.422
64	Angelina	59	E	2.682	0.1251	1.31	309.0	179.7	133.8	4.393	8.752
170	Maria	46	S	2.552	0.0648	14.43	300.9	157.4	242.3	4.078	
446	Aeternitas	43	A	2.787	0.1267	10.62	41.8	279.6	167.7	4.652	
1036	Ganymed	41	S	2.665	0.5366	26.45	215.6	131.7	343.7	4.350	10.308
158	Koronis	39	S	2.870	0.0521	1.00	278.1	142.5	187.0	4.861	14.18
243	Ida	32	S	2.863	0.0421	1.14	323.9	110.6	203.5	4.843	4.65

Table 15. (cont) Prominent Minor Planets or Asteroids

No.	Name	Dia. km	Tax	<i>a</i> AU	<i>e</i>	<i>I</i> deg	Ω deg	ω deg	<i>M</i> deg	Period year	Rotation hrs
433	Eros	20	S	1.458	0.2229	10.83	303.7	178.6	122.1	1.761	5.270
951	Gaspra	14	S	2.210	0.1737	4.10	252.7	129.4	52.9	3.286	7.042
434	Hungaria	10	E	1.944	0.0740	22.51	174.8	123.8	258.3	2.711	26.51

Table 15: Size, Orbits and rotation periods [35] of prominent objects. This table is sorted by size which are largely determined from the visual and infrared (from IRAS) magnitudes, although a few are from stellar occultations and other sources. All objects with diameters larger than 200 km are included. A few smaller objects are included because of unusual characteristics or because they are Galileo fly-by targets (951 Gaspra and 243 Ida, a Koronis family member). 24 Themis, 221 Eos, 158 Koronis, 170 Maria and 8 Flora are prominent representatives of major asteroid families of collision fragments. The low perihelion distances (usually denoted $q = a(1 - e)$) for 433 Eros ($q = 1.133\text{AU}$)

and 1036 Ganymed ($q = 1.234\text{AU}$) indicate that they are Mars' crossers. 2060 Chiron is in a distant, comet-like orbit. Initially a point source, it was catalogued as an asteroid, but subsequently exhibited cometary activity as it approached perihelion. There is no secure diameter measurement, although its brightness indicates a large diameter of several hundred km. The three largest asteroids have rare or unusual taxonomies. The epoch for the orbit parameters is Oct. 1, 1989, although they are referenced to the 1950 equinox and ecliptic (table and notes from J. G. Williams).

*: Periods are uncertain or controversial.

Table 16. Near Earth Asteroids

No	Name	Dia. km	P_v	Rot. hrs	<i>q</i> AU	<i>e</i>	<i>I</i>	Encounter date(dist.in AU)
2062	Aten	0.9	0.20		0.790	0.183	18.9	1/12/95(0.127)
2100	Ra-Shalom	2.4	0.09	19.79	0.469	0.437	15.8	9/26/97(0.171)
2063	Bacchus				0.701	0.350	9.4	3/31/96(0.068)
2340	Hathor				0.464	0.450	5.9	10/25/00(0.197)
3362	Khufu	0.7	0.16		0.526	0.469	9.9	1/24/00(0.293)
3554	Amun	2.0	0.17		0.700	0.281	23.4	
1862	Apollo	1.5	0.21	3.065	0.647	0.560	6.35	
1566	Icarus	0.9	0.42	2.273	0.187	0.827	22.9	6/11/96(0.101)
1620	Geographos	2.0	0.19	5.227	0.827	0.336	13.3	8/25/94(0.033)
1685	Toro	5.2	0.14	10.196	0.771	0.436	9.4	8/02/96(0.221)
1863	Antinous	1.8	0.18	4.02	0.890	0.606	18.4	4/10/99(0.190)
1865	Cerberus	1.0	0.26	6.80	0.576	0.467	16.1	11/24/98(0.163)
1866	Sisyphus	8.2	0.18		0.873	0.539	41.2	
2102	Tantalus				0.905	0.299	64.0	12/21/97(0.138)
2201	Oljato	1.4	0.42	> 24.0	0.905	0.299	64.0	
3103	1982 BB				0.907	0.354	20.9	8/06/96(0.115)
3200	Phaethon	6.9	0.08		0.140	0.890	22.1	
4179	Toutatus				0.921	0.634	0.5	11/29/96(0.035)
4183	Cuno				0.718	0.637	6.8	12/22/00(0.143)
4197	1982 TA				0.522	0.773	12.2	10/25/96(0.085)
4486	1987 SB				0.743	0.663	3.0	8/14/00(0.047)
	1988 EG				0.636	0.499	3.9	2/28/98(0.032)
	1986 JK				0.896	0.680	2.1	7/11/00(0.122)
4034	1986 PA				0.589	0.444	11.2	8/28/97(0.206)

TABLE 16. (continued).

No	Name	Dia. km	P_v	Rot. hrs	q AU	e	I	Encounter date(dist.in AU)
4769	Castelia				0.550	0.483	8.9	4/08/93(0.132)
433	Eros	22	0.18	5.27	1.133	0.223	10.83	
887	Alinda	4.2	0.23	73.97	1.101	0.560	9.27	
1036	Ganymed	38.5	0.17	10.31	1.229	0.539	26.6	
1580	Betulia	7.4	0.03	6.13	1.119	0.490	52.1	
1627	Ivar	8.1	0.12	4.80	1.124	0.397	8.4	
1980	Tezcatlipoca	4.3	0.21		1.085	0.365	26.9	11/16/97(0.274)
3102	1981 QA			148	1.189	0.447	8.4	
3288	Seleucus	2.8	0.17	75.	1.103	0.457	5.9	
3361	Orpheus	0.8			0.819	0.323	2.7	2/12/98(0.167)
3552	Don Quixote	18.7	0.02		1.212	0.714	30.8	
3671	Dionysius				1.003	0.543	13.6	7/06/97(0.114)
3908	1982 PA				1.056	0.317	10.8	10/27/96(0.061)

Table 16: Prominent Aten, Apollo, and Amor class near earth asteroids. Orbit elements ($q \equiv a(1-e)$), e , inclination I , date (mm/dd/yr) of closest approach to earth and corresponding minimum separation (in AU) during the 1993-2000 time period are from D. Yeomans (priv. comm.). These are

taken from a list of 85 objects with well determined orbits for which the estimated population is over 4000 ($V(1,0) < 18$). The size, visual albedo (P_v) and rotation period are given if known [72].

Table 17. Asteroid Mass Determinations

Object	Mass 10^{22} g	Diam. km	density g cm^{-3}	ref.
Ceres	117 \pm 6	940	2.7	a
	104 \pm 6		2.4	b
	99 \pm 4		2.3	c
Pallas	22 \pm 4	538	2.6	a
	28 \pm 4		3.4	c
Vesta	28 \pm 2	525	3.6	a
	30 \pm 6		3.9	c
Hygeia	9 \pm 4	427	2.3	c

Table 17: Masses and densities exist for only four large asteroids. These masses result from tracking their orbital perturbation of other asteroids (a,b,d) detected from ground-based astrometry: (a) Schubart [94], (b) Landgraf [63], (c)

Scholl *et al.* [93] or radio tracking of Viking Mars' landers (d) Standish and Hellings [102], and from which these results were obtained.

Table 18. Prominent Short Period Comets: Epoch B1950

Comet	l deg	ω deg	Ω deg	I deg	e	a AU	T_p JD	M_1	M_2
Arend	359.75	47.06	355.49	19.929	0.53703	3.9961	2448402.5	9.5	15.0
Arend-Rigaux	358.31	329.06	121.45	17.888	0.60005	3.5950	2448532.2	10.0	15.5
Ashbrook-Jackson	2.36	348.69	1.97	12.494	0.39491	3.8279	2449182.5	1.0	11.5
Boethin	0.36	22.31	13.74	4.871	0.77436	5.1329	2450556.2	10.0	14.0
Borrelly	359.03	353.36	74.74	30.323	0.62390	3.6112	2452167.2	4.5	13.0
Brooks 2	0.56	197.99	176.25	5.548	0.49073	3.6196	2449596.5	9.0	13.5
Brorsen-Metcalf	0.27	129.62	310.88	19.331	0.99196	17.073	2447781.4	7.8	14.0
Churyumov-									
Gerasimenko	3.04	11.34	50.35	7.110	0.63021	3.5156	2450100.1	9.5	14.5
Comas Solá	359.50	45.74	60.20	12.914	0.56779	4.2719	2450244.9	8.0	12.5
Crommelin	359.36	195.99	249.93	28.959	0.91875	9.2046	2455778.5	12.0	16.0
d'Arrest	359.19	178.04	138.30	19.528	0.61404	3.4871	2449925.8	8.5	16.0
Denning-Fujikawa	0.43	337.56	35.72	9.130	0.81792	4.3372	2450236.5	15.0	19.0
du Toit-Hartley	3.48	251.57	308.56	2.938	0.60161	3.0050	2448862.1	14.0	18.0
Encke	1.00	186.49	333.89	11.750	0.84690	2.2177	2451797.1	9.8	14.5
Faye	357.83	203.95	198.88	9.091	0.57818	3.7774	2448576.6	8.0	14.0
Finlay	359.70	323.47	41.42	3.669	0.71030	3.5746	2449842.5	12.0	17.0
Forbes	2.88	310.72	333.65	7.16	0.56811	3.3481	2451302.5	10.5	15.5
Gehrels 2	1.77	192.80	209.90	6.263	0.46357	3.7289	2450667.6	5.5	13.0
Giacobini-									
Zinner	359.22	172.52	194.68	31.828	0.70649	3.5229	2448725.7	9.0	15.5
Grigg-Skjellerup	2.87	359.27	212.63	21.104	0.66433	2.9633	2448825.6	12.5	17.0
Gunn	358.78	196.79	67.86	10.378	0.31632	3.6010	2450288.9	5.0	10.0
Halley	0.12	111.85	58.14	162.239	0.96728	17.9415	2446470.9	5.5	13.0
Hartley 2	359.41	180.74	219.24	13.63	0.70037	3.4432	2450804.3	10.5	14.5
Honda-Mrkos-									
Padušáková	0.39	326.05	88.48	4.257	0.82512	3.0211	2451998.3	13.5	18.0
Kopff	2.11	162.76	120.28	4.724	0.54408	3.4645	2450266.6	3.0	13.5
Olbers	359.84	64.41	85.16	44.67	0.93031	16.8666	2460491.9	5.0	11.5
Pons-Winnecke	359.31	172.30	92.75	22.302	0.63443	3.4354	2450084.9	10.0	16.0
Schaumasse	358.79	57.45	80.39	11.846	0.70487	4.0734	2449050.6	9.0	15.5
Schwassmann-									
Wachmann 2	358.59	18.33	113.57	4.552	0.19529	4.2357	2452292.9	7.6	14.0
Tempel 2	1.91	195.00	117.54	11.980	0.52282	3.1051	2451429.9	4.0	15.0
Tempel-Tuttle	0.24	172.52	234.58	162.49	0.90551	10.335	2450872.5	9.0	13.0
Tuttle-Giacobini-									
Kresák	358.80	61.68	140.82	9.230	0.65642	3.1003	2449927.1	10.0	18.0
Wild 2	357.74	41.70	135.53	3.248	0.54023	3.4422	2450575.1	6.5	13.0
Wirtanen	0.06	356.15	81.61	11.683	65225	3.1152	2448520.1	9.0	15.5
Wolf	2.13	162.29	203.44	27.483	0.40560	4.0843	2448862.6	10.0	16.0

Table 18: This list of short period comets (period <200 yr) has been drawn from a much larger list compiled by D. Yeomans (priv. comm.) and are themselves primarily taken from Minor Planet Circulars (also see [117]). The material includes orbital data (epoch 1950): a , e , I , ℓ , ω , Ω , the Julian date of perihelion passage and the absolute (M_1) and nu-

clear (M_2) magnitudes. All comets are affected by nongravitational forces related to sublimation of ices (H_2O , CO_2 , N_2 , NH_3 , etc.) which can significantly change the orbit over time, especially the timings of perihelion passage. Some asteroids such as 944 Hidalgo may be extinct comets.

Table 19. Sun: Physical Properties

GM_{\odot}	$1.327124399(4 \pm 5) \times 10^{11} \text{ km}^3 \text{ s}^{-2}$
Mass	$1.9891 \times 10^{30} \text{ kg}$
Radius ^a (photosphere)	$6.960 \times 10^5 \text{ km}$
Angular diameter at 1 AU	$1919''.3''$
Mean density	1.408 g cm^{-3}
Surface gravity	274.0 m s^{-2}
Moment of inertia I/MR^2	0.059
Escape velocity $v_{\infty} = \sqrt{2GM/R}$	617.7 km s^{-1}
Adopted sidereal period ^b	25.38d
Pole: (RA Dec)	$\alpha = 286.13^\circ; \delta = 63.87^\circ$
Obliquity to ecliptic	$7^\circ 15'$
Longitude of ascending node	$75^\circ 46' + 84' T$
Surface rotation rate ^a ν as function of latitude ϕ	$(\nu = 462 - 75 \sin^2 \phi - 50 \sin^4 \phi) \text{ nHz}$ $(462 \text{ nHz} = 14.37^\circ \text{ d}^{-1})$
Solar constant (1 AU) ^f	1367.6 W m^{-2}
Solar luminosity L_{\odot}	$3.846 \times 10^{33} \text{ ergs s}^{-1}$
Mass-energy conversion rate	$4.3 \times 10^{12} \text{ gm s}^{-1}$
Effective temperature $= (L_{\odot}/\sigma_{SB})^{1/4}$	5778°K
Surface Temperature (photosphere) ^a	$6600^\circ \text{K}(\text{bottom}); 4400^\circ \text{K}(\text{top})$
Motion relative to nearby stars ^c	apex: $\alpha = 271^\circ; \delta = +30^\circ$ speed: $19.4 \text{ km s}^{-1} = 0.0112 \text{ AU d}^{-1}$
Motion relative to 2.73°K BB deduced from thermal dipole ^d	$369 \pm 11 \text{ km s}^{-1}$ apex: $l = 264^\circ 7 \pm 0.8; b = 48^\circ 2 \pm 0.5$
Sun spot cycle	11.4yr
Cycle 22 solar sunspot maximum	1991
Photospheric depth ^a	$\simeq 400 \text{ km}$
Chromospheric depth	$\sim 2500 \text{ km}$

Table 19: See Cox *et al.* [26] for general summary of solar science. References: a) Alcock [2]; b) Davies *et al.* [29]; c) Allen [1]; d) Smoot *et al.* [99]; e) SMM/ACRIM

result [70]. The solar constant varies by 0.04% during a solar cycle. During solar maximum, sunspots can change the solar constant by 1/4% during one rotation.

Table 20. Solar Interior Model

M_r/M_R	r/R)	Pressure dyne cm $^{-2}$	Temp. 10 6 K	Density g cm $^{-3}$	L_r/L_R L_R
0.0000	0.0000	$2.477 + 17$	15.710	162.2	0.0000
0.0103	0.0462	$2.144 + 17$	15.010	138.4	0.0819
0.0406	0.0766	$1.716 + 17$	14.000	110.6	0.2766
0.1026	0.1116	$1.234 + 17$	12.650	81.64	0.5514
0.2023	0.1520	$7.889 + 16$	11.100	56.62	0.7969
0.3036	0.1873	$5.108 + 16$	9.864	40.34	0.9150
0.4051	0.2216	$3.248 + 16$	8.803	28.42	0.9683
0.4981	0.2546	$2.066 + 16$	7.920	20.01	0.9896
0.5985	0.2943	$1.182 + 16$	7.012	12.93	0.9983
0.6979	0.3419	$6.048 + 15$	6.114	7.584	0.9999
0.7991	0.4073	$2.460 + 15$	5.138	3.679	1.0002
0.8989	0.5129	$6.198 + 14$	4.594	1.231	1.0002
0.9504	0.6177	$1.731 + 14$	3.082	0.4386	1.0001
0.9803	0.7363	$4.203 + 13$	2.031	0.1604	1.0001
0.9951	0.8489	$7.059 + 12$	1.000	0.0549	1.0001
0.9999	0.9634	$9.941 + 10$	0.190	0.0043	1.0001

Table 20: Standard model by Cox, Gudzik and Kidman [26] which constrains the metallicity factor $Z = 0.02$ and the helium mass fraction to $Y = 0.291$. Competing “standard”

models [45] differ for internal radius $< 0.1R_\odot$ and which have 10% lower central pressure and density.

a: Pressure column reads: $2.477 + 17 = 2.477 \times 10^{17}$.

Table 21. Solar Luminosity History

t Gyr	$R(t)/R(4.6)$	T_c 10 6 K	ρ_c g cm $^{-3}$	T_{eff} K	$L(t)/L(4.6)$
0.00	0.8755	13.69	81.44	5649	0.7044
0.50	0.8939	13.75	90.19	5678	0.7496
1.00	0.9050	13.92	95.55	5692	0.7745
1.50	0.9153	14.12	101.5	5704	0.8000
2.00	0.9268	14.32	108.3	5717	0.8262
2.50	0.9386	14.54	115.6	5729	0.8561
3.00	0.9516	14.78	124.3	5741	0.8872
3.50	0.9651	15.04	133.8	5750	0.9185
4.00	0.9801	15.32	145.2	5761	0.9539
4.64	1.0000	15.71	162.2	5770	1.0000

Table 21: Evolution of solar luminosity, radius, central temperature T_c , pressure P_c and density ρ_c , from solar ignition at zero age to the present at 4.6 Gy [26]. Note that

the increase in luminosity is primarily due to a change in photospheric radius.

Acknowledgements. I wish to thank to a variety of individuals who contributed material or reviewed this paper, including J. Campbell, R. Gross, A. Harris, A. Konopliv, D. Nicholson, G. Null, W. Owen Jr., N. Rappaport, M. Stansfield, S. Synnott, P. Thomas, J. Wahr, J. G. Williams and

D. Yeomans, but not excluding many others. This paper presents the results of one phase of research carried out at the Jet Propulsion Laboratory, California Institute of Technology, under NASA Contract NAS 7-100, supported by the National Aeronautics and Space Administration.

REFERENCES

1. Allen, C. W., *Astrophysical Quantities* (3rd ed.), Atholone Press, London, 310pp, 1985.
2. Altrock, R. C., H. L. DeMastus, J. W. Evans, S. L. Keil, D. F. Neidig, R. R. Radick, R. R. and G. W. Simon, The Sun, in *Handbook of Geophysics and the Space Environment*, edited by A. S. Jursa, Air Force Geophysics Laboratory, 1.1-1.25, 1985.
3. Anderson, J. D., G. Colombo, P. B. Esposito, E. L. Lau and G. B. Trager, The mass and gravity field of Mercury, *Icarus*, 71, 337-349, 1987.
4. Avensov, G. A. et al, Television observations of Phobos, *Nature*, 341, 585-587, 1989.
5. Balmino, G., B. Moynot and N. Vales, Gravity Field of Mars in spherical harmonics up to degree and order 18, *J. Geophys. Res.*, 87, 9735-9746, 1982.
6. Baron, R. L., R. G. French, and J. L. Elliot, The oblateness of Uranus at the $1-\mu\text{bar}$ level, *Icarus*, 78, 119-130, 1989.
7. Basaltic Volcanism Study Project, *Basaltic Volcanism on the Terrestrial Planets*, Pergamon Press, New York, 1286pp., 1981.
8. Batson, R. M., K. Edwards and T. C. Duxbury, Geodesy and Cartography of the Martian satellites, in *Mars*, edited by H. H. Kieffer, B. M. Jakosky, C.W. Snyder and M. S. Matthews, Univ. of Arizona Press, Tucson, 1992.
9. Bills, B. G. and A. J. Ferrari, A harmonic analysis of lunar topography, *Icarus*, 31, 244-259, 1977.
10. Bills, B. G. and A. J. Ferrari, Mars' topography harmonics and geophysical implications, *J. Geophys. Res.*, 83, 3497-3508, 1978.
11. Bills, B. G. and M. Kobrick, Venus topography: a harmonic analysis, *J. Geophys. Res.*, 90, 827-836, 1985.
12. Borderies, N. and C. F. Yoder, Phobos' gravity field and its influence on its orbit and physical librations, *Astron. Astrophys.*, 233, 235-251, 1990.
13. Brouwer, D. and G. M. Clemence, *Methods of Celestial Mechanics*, Academic Press, New York, 598pp, 1961.
14. Burns, J. A., Some background about satellites, in *Satellites*, edited by J. A. Burns and M. S. Matthews, Univ. of Arizona Press, Tucson, 1-38, 1986.
15. Buie, M. W., D. J. Tholen and K. Horne, Albedo maps of Pluto and Charon: initial mutual event results, *Icarus*, 97, 211-227, 1992.
16. Campbell, J. K. and S. P. Synnott, Gravity field of the jovian system from pioneer and voyager tracking, *Astron. J.*, 90, 364-372, 1985.
17. Campbell, J. K. and J. D. Anderson, Gravity field of the Saturnian system from Pioneer and Voyager tracking data, *Astron. J.*, 97, 1485-1495, 1989.
18. Caputo, M., The minimum strength of the earth, *J. Geophys. Res.*, 70, 953-963, 1965.
19. Cartwright, D. E. and R. D. Ray, Oceanic tides from Geosat, *J. Geophys. Res.*, 95, 3069-3090, 1990.
20. Chandrasekhar, S., *Ellipsoidal Figures of Equilibrium*, Yale Univ. Press, New Haven, CN, 1969.
21. Chapront-Touze, M., and J. Chapront, ELP2000-85: a semianalytic lunar ephemeris adequate for historical times, *Astron. Astrophys.*, 190, 342-352, 1988.
22. Cheng, M. K., R. J. Eanes and B. D. Tapley, Tidal deceleration of the Moon's mean motion, *Geophys. J.*, 108, 401-409, 1991.
23. Clark, C. R. and R. O. Vicente, Maximal likelihood estimates of polar motion parameters, in *Variations in earth rotation*, edited by D. D. McCarthy and W. E. Carter, American Geophysical Union monograph, 151-155, 1990.
24. Cook, A. H., The external gravity field of a rotating spheroid to the order of e^3 , *Geophys. J. R. Astr. Soc.*, 2, 199-214, 1959.
25. Connerney, J. E. P., L. Davis Jr. and D. L. Chenette, in *Saturn*, edited by T. Gehrels and M. S. Matthews , Univ. of Arizona Press, Tucson, 354-377, 1984.
26. Cox, A. N., W. C. Livingston and M. S. Matthews, *Solar Interior and Atmosphere*, Univ. of Arizona Press, Tucson, 1416pp, 1991.
27. Davies, M. E., P. G. Rogers and T. R. Colvin, A control network of Triton, *J. Geophys. Res.*, 96, 15675-15681, 1991.
28. Davies, M. E., V. K. Abalkin, A. Brahic, M. Bursa, B. H. Chovitz, J. H. Lieske, P. K. Seidelmann, A. T. Sinclair and Y. S. Tjuflin, Report of the IUA/IAG/COSPAR working group on cartographic coordinates and rotational elements of the planets and satellites: 1991, *Icarus*, 93, 377-397, 1992.
29. Davies, M. E. and 8 authors, The rotation period, direction of the north pole, and geodetic control network of Venus, *J. Geophys. Res.*, 97, 13141-13151, 1992.
30. Dermott, S. F. and P. C. Thomas, The shape and internal structure of Mimas, *Icarus*, 73, 25-65, 1988.
31. Dermott, S. F. and P. C. Thomas, Shapes, masses and interiors of satellites, *Adv. Space Res.*, 10, 165-172, 1990.
32. Dickey, J. O., P. L. Bender, J. E. Faller, X X Newhall, R. L. Ricklets, J. G. Ries, P. J. Shelus, C. Veillet, A. L. Whipple, J. R. Wiant, J. G. Williams and C. F. Yoder, Lunar laser ranging: A continuing legacy of the Apollo Program, *Science*, 265, 482-490, 1994.
33. Duxbury, T. C., An analytic model for the Phobos surface, *Planet. Space Sci.*, 39, 355-376, 1991.
34. Elliot, J.L. and L. A. Young, Analysis of stellar occultation data for planetary atmospheres. I: model fitting, with application to Pluto, *Astron. J.*, 103, 991-1015, 1992.
35. Ephemerides of the minor planets for 1993, Russian Academy of Sciences, Institute for Theoretical Astronomy, edited by Y. V. Batrakov, St. Petersburg, 511pp, 1992.
36. Esposito, L. W., C. C. Harris and K. E. Simmons, Features in Saturn's rings, *Astrophys. J. Suppl.*, 63, 749-

- 770, 1987.
37. Esposito, P. B., W. B. Banerdt, G. F. Lindal, W. L. Sjogren, M. A. Slade, B. G. Bills, D. E. Smith and G. Balmino, Gravity and Topography, in *Mars*, edited by H. H. Kieffer, B. M. Jakosky, C. W. Snyder and M. S. Matthews, Univ. of Arizona Press, Tucson, 209-248, 1992.
38. Ferrari, A. J., W. S. Sinclair, W. L. Sjogren, J. G. Williams and C. F. Yoder, Geophysical Parameters of the earth-moon system, *J. Geophys. Res.*, **85**, 3939- 3951, 1980.
39. French, F. G., J. L. Elliot, L. M. French, K. J. Meech, M. E. Ressler, M. W. Buie, J. A. Frogel, J. B. Holberg, J. J. Fuensalida and M. Joy, Uranian ring orbits from Earth-based and Voyager occultation data, *Icarus*, **73**, 349-378, 1988.
40. French, R. G. et al., Uranian ring orbits from Earth-based and Voyager occultation observations, *Icarus*, **73**, 349-378, 1988.
41. French, R. G., P. D. Nicholson, C. C. Porco and E. A. Marouf, Dynamics of the Uranian rings, in *Uranus* edited by J. T. Bergstrahl, E. D. Miner and M. S. Matthews, Univ. Arizona Press, Tucson, 327-409, 1991.
42. French, R. G. et al., Geometry of the Saturn system from the 3 July 1989 occultation of 28 Sgr and Voyager observations, *Icarus*, **103**, 1993.
43. Gaskell, R. W., S. P. Synnott, A. S. McEwen and G. G. Schaber, Large scale topography of Io: implications for internal structure and heat transfer, *Geophys. Res. Letters*, **15**, 581-584, 1988.
44. Goins, N. , A. M. Dainty and M. N. Toksoz, Lunar Seismology: the internal structure of the moon, *J. Geophys. Res.*, **86**, 5061-5074, 1981.
45. Guzik, J. A. and Y. Lebreton, Solar interior models, in *Solar Interior and Atmosphere*, edited by A. N. Cox, W. C. Livingston and M. S. Matthews, Univ. of Arizona Press, Tucson, 1235-1248, 1991.
46. Harmon, J. K., J. B. Campbell, D. L. Bindschadler, J. W. Head and I. I. Shapiro, Radar altimetry of Mercury: a preliminary analysis, *J. Geophys. Res.*, **91**, 385-401, 1986.
47. Harper D. and D. B. Taylor, The orbits of the major satellites of Saturn, *Astron. Astrophys.*, in press, 1993.
48. Heiken, G. H., D. V. Vaniman and B. M. French *Lunar Sourcebook*, Cambridge University Press and L.P.I., Houston Tx, 1993.
49. Herring, T. A., B. A. Buffett, P. M. Mathews and I. I. Shapiro, Forced nutations of the earth: influence of inner core dynamics 3. Very long interferometry data analysis, *J. Geophys. Res.*, **96**, 8259-8273, 1991.
50. Hubbard, W. M. and R. Smoluchowski, Structure of Jupiter and Saturn, *Space Sci. Rev.*, **14**, 599-662, 1973.
51. Hubbard, W. M. , Effects of differential rotation on the gravitational figures of Jupiter and Saturn, *Icarus*, **52**, 509-515, 1982.
52. Hubbard, W. B. and M. S. Marley, Optimized Jupiter, Saturn and Uranus Interior models, *Icarus*, **78**, 102-118, 1989.
53. Jacobson, R. A., J. E. Riedel and A. H. Taylor, The orbits of Triton and Nereid from spacecraft observations, *Astron. Astrophys.*, **247**, 565-575, 1991.
54. Horn, L. J., J. Hui, A. L. Lane, R. M. Nelson and C. T. Russell, Saturn A ring surface mass densities from spiral density wave dispersion behavior, *Icarus*, in press, 1993.
55. Jacobson, R. A., J. K. Campbell, A. H. Taylor and S. P. Synnott, The masses of Uranus and its major satellites from Voyager tracking data and earth-based Uranian satellite data, *Astron. J.*, **103**, 2068-2078, 1992.
56. Jefferies, H., *The Earth*, Cambridge University Press, Cambridge, 574pp, 1976.
57. Kaula, W. M., *Theory of satellite geodesy*, Blaisdell, Waltham, 124pp, 1966.
58. Kaula, W. M., *An Introduction to Planetary Physics*, John Wiley & Sons, New York, 490pp, 1968.
59. Klevettet, J. G., Rotation of Hyperion. II dynamics, *Astron. J.*, **98**, 1855-1874, 1989.
60. Konopliv, A. S., N. J. Borderies, P. W. Chodas, E. J. Christensen, W. L. Sjogren, G. Balmino and J. P. Barriot, Venus gravity and topography: 60th degree and order field, *Geophysical Res. Lett.*, in press, 1993.
61. Konopliv, A. S., W. L. Sjogren, R. N. Wimberly, R. A. Cook and A. Vijayaraghavan, A high resolution lunar gravity field and predicted orbit behavior, *AAS/AIAA Astrodynamics Conf.*, AIAA/AAS, 93-622, Victoria BC, 1993.
62. Lambeck, K., *The earth's variable rotation*, Cambridge university press, Cambridge, 449pp, 1980.
63. Landgraf, W., The mass of Ceres, *Astron. Astrophys.*, **191**, 161-166, 1988.
64. Laskar, J. and P. Robutel, The chaotic obliquity of the planets, *Nature*, **361**, 608-612, 1993.
65. Lieske, J. H., Galilean satellite evolution: observational evidence for secular changes in mean motion, *Astron. Astrophys.*, **176**, 146-158, 1988.
66. Lindal, G. F., The atmosphere of Jupiter: an analysis of the radio occultation measurements, *J. Geophys. Res.*, **86**, 8721-8727, 1981.
67. Lindal, G. F., D. N. Sweetnam and V. R. Eshelman, The atmosphere of Saturn: an analysis of the Voyager radio occultation measurements, *Astron. J.*, **90**, 1136-1146, 1985.
68. Lindal, G. F., J. R. Lyons, D. N. Sweetnam, V. R. Eshelman, D. P. Hinson and G. L. Tylor, The atmosphere of Uranus: results of radio occultation measurements with Voyager 2, *J. Geophys. Res.*, **92**, 14,987-15,001, 1987.
69. Lindal, G. F., An analysis of radio occultation data aquired with Voyager 2, *Astron. J.*, **103**, 967-982, 1992.
70. Livingston, W., R. F. Donnelly, V. Grioryev, M. L. Demidov, J. Lean, M. Steffan, O. R. White and R. L. Willson, Sun as a star spectrum variability, in *Solar interior and Atmosphere*, edited by A. N. Cox, W. C. Livingston and M. S. Matthews, Univ. of Arizona Press, Tucson, 1109-1160, 1991.
71. Marsh, J. G., F. J. Lerch, B. H. Putney, T. L. Felsentreger, B. V. Sanchez, S. M. Klosko, G. B. Patel,

- J.W. Robbins, R. G. Williamson, T. L. Englisch, W. F. Eddy, N. L. Chandler, D. S. Chinn, S. Kapoor, K. E. Rachlin, L. E. Braatz and E. C. Pavlis, The GEM-T2 gravitational model, *J. Geophys. Res.*, 95, 22043-22071, 1990.
72. McFadden, L. A., D. J. Tholen and G. J. Vedder, Physical properties of Aten, Apollo and Amor Asteroids, in *Asteroids II*, edited by R. P. Binzel, T. Gehrels and M. S. Matthews, Univ. of Arizona Press, Tucson, 1258pp, 1992.
73. McNamee, J.B., N. J. Borderies, W. L. Sjogren, Global Gravity and Topography, *J. Geophys. Res., Planets*, 98, 9113-9128, 1993.
74. Moritz, H., Geodetic reference system 1980, in *The Geodesist's Handbook: 1984*, edited by C. C. Tscherning, 58, 1984.
75. Morrison, L. V. and C. G. Ward, *Mon. Not. Roy. astr. Soc.*, 173, 183, 1975.
76. Nakamura, Y., G. V. Latham and H. J. Dorman, Apollo lunar seismic experiment - final summary, *J. Geophys. Res.*, 87, a117-a123, 1981.
77. Nakamura, Y., Seismic velocity structure of the lunar mantle, *J. Geophys. Res.*, 88, 677-686, 1983.
78. Ness, F.N., M. H. Acuna, L. F. Burlaga, J. E. P. Connerney, and F. M. Lepping, Magnetic Fields at Neptune, *Science*, 246, 1473-1477, 1989.
79. Nicholson, P.D. and C.L. Porco, A new constraint on Saturn's zonal gravity harmonics from Voyager observations of an eccentric ringlet, *J. Geophys Res.*, 93, 10209-10224, 1988.
80. Nicholson, P. D. and L. Dones, Planetary Rings, *Rev. of Geophysics*, 313-327, 1991.
81. Nicholson, P. D., D. P. Hamilton, K. A. Matthews and C. F. Yoder, New observations of Saturn's coorbital satellites, *Icarus*, 100, 464-484, 1993.
82. Null, G. W., E. L. Lau, E. D. Biller and J. D. Anderson, Saturn Gravity results obtained from Pioneer 11 tracking data and Earth-based Saturn satellite data, *Astron. J.*, 86, 456-468, 1981.
83. Null, G. W., W. M. Owen Jr., S. P. Synnott, Masses and densities of Pluto and Charon, *Astron. J.*, 105, 2319, 1993.
84. Owen, W. M. Jr. and S. P. Synnott, Orbits of the ten small satellites of Uranus, *Astron. J.*, 93, 1268-1271, 1987.
85. Owen, W. M. Jr., A theory of the earth's precession relative to the invariable plane, PhD Thesis, University of Florida, 1990.
86. Owen, W. M. Jr., R. M. Vaughan and S. J. Synnott, Orbits of the six new satellites of Neptune, *Astron. J.*, 101, 1511-1515, 1991.
87. Peale, S. J., Generalized Cassini Laws, *Astron. J.*, 74, 483-489, 1969.
88. Plummer, H. C., *An Introductory Treatise on Dynamical Astronomy*, Dover, New York, 343pp. 1960.
89. Podolak, M. B., W. M. Hubbard and D. J. Stevenson, Models of Uranus' interior and magnetic field, in *Uranus*, edited by J. T. Bergstrahl, E. D. Miner and M. S. Matthews, Univ. Arizona Press, Tucson, 29-61, 1991.
90. Rapp, R. H., Current estimates of the mean earth ellipsoid parameters, *Geophys. Res. Lett.*, 1, 35-38, 1974.
91. Rosen, P. A., G. L. Tyler, E. F. Marouf and J. J. Lissauer, Resonance structures in Saturn's rings probed by radio occultation, *Icarus*, 92, 25-44, 1991.
92. Russell, C. T., P. J. Coleman Jr. and B. E. Goldstein, Measurements of the lunar induced magnetic moment in the geomagnetic tail: evidence for a lunar core, *Proc. Lunar Planet. Sci.*, 12B, 831-836, 1981.
93. Scholl, H., L. D. Schmadel and S. Roser, The mass of the asteroid(10) Hygeia derived from observations of (829) Academia, *Astron. Astrophys.*, 179, 311-316, 1987.
94. Schubart, J., The mass of Pallas, *Astron. Astrophys.*, 39, 147-148, 1975.
95. Seidelmann, P. K. (editor), *Explanatory supplement to the astronomical almanac*, University Science Books, Mill Valley, 752pp, 1992.
96. Sellers, P. C., Seismic Evidence for a low-velocity lunar core, *J. Geophys. Res.*, 97, 11663-11672, 1992.
97. Sinclair, R. A., The orbits of the satellites of Mars from spacecraft and ground-based observations, *Astron. Astrophys.*, 220, 321-328, 1989.
98. Smart, W. M., *Celestial Mechanics*, John Wiley, New York, 381pp, 1961.
99. Smoot, G. F. plus 27 authors, Structure in the COBE differential microwave Radiometer first year maps, *Astrophys. J.*, 396, L1-L6, 1992.
100. Souchay, J. and H. Kinoshita, Comparison of new nutation series with numerical integration, *Cel. Mech.*, 52, 45-55, 1991.
101. Stacey, F.D., *Physics of the Earth*, John Wiley, New York, 414pp, 1977.
102. Standish, E. M. jr. and R. W. Hellings, A determination of the masses of Ceres, Pallas and Vesta from their perturbations upon the orbit of Mars, *Icarus*, 80, 326-333, 1989.
103. Standish, E. M., The observational basis for JPL's DE 200, the planetary ephemerides of the Astronomical Almanac, *Astron. Astrophys.*, 233, 252-271, 1990.
104. Synnott, S. P., R. J. Terrile, R. A. Jacobson and B. A. Smith, Orbits of Saturn's F-Ring and its shepherding satellites, *Icarus*, 53, 156-258, 1983.
105. Synnott, S. P., Orbits of the small satellites of Jupiter, *Icarus*, 58, 178-181, 1984.
106. Thomas, P. C., C. Weitz and J. Neverka, Small satellites of Uranus: Disk-integrated photometry and estimated radii, *Icarus*, 81, 92-101, 1989.
107. Thomas, P. C., The shape of small satellites, *Icarus*, 77, 248-274, 1989.
108. Thomas, P. C. and S. F. Dermott, The Shape of Tethys, *Icarus*, 94, 391-398, 1991.
109. Torge, W., *Geodesy*, Walter de Gruyter, New York, 254pp, 1980.
110. Turcotte, D. L. and G. Schubart, *Geodynamics*, John Wiley & Sons, New York, 450pp, 1982.
111. Tyler, G. L. and 17 authors, Radio Science observations of Neptune and Triton, *Science*, 246, 1466-1473, 1989.
112. Ward, W. R. and D. Jurdy, Resonant Obliquity of Mars?, *Icarus*, 94, 160-164, 1991.

113. Williams, J. G., W. S. Sinclair and C. F. Yoder, *Geophys. Res. Lett.*, 5, 943-946, 1978.
114. Williams, J. G., X X Newhall and J. O. Dickey, Lunar gravitational harmonics and the reflector coordinates, in *Proc. Int. Symp. Figure and Dynamics of the Earth, Moon and Planets, Prague, 1986*, Hotola, P. ed., 643-648 , 1987.
115. Williams, J. G. , X. X. Newhall and J. O. Dickey, Diurnal and semidiurnal contributions to lunar secular acceleration, *EOS*, 73, 126, 1992.
116. Williams, J. G., Contributions to the earth's obliquity rate, precession and nutation, *Astron. J.*, 108, 711-724, 1992.
117. Yeomans, D. and R. N. Wimberly, Cometary apparitions: 1990-2011, in *Comets in the Post-Halley Era: Vol. II*, edited by R. L. Newburn, M. Neugebauer and J. Rahe, 1281-1308, 1991.
118. Yoder, C. F. and W. R. Ward, Does Venus wobble?, *Ap. J. Letters*, 233, L33-L37, 1979.
119. Yoder, C. F.,The free librations of a dissipative moon, *Philos. Trans. R. Soc. London Ser. A*, 303, 327-338, 1981.
120. Yoder, C. F., The tidal rigidity of Phobos, *Icarus*, 49, 327-345, 1982.
121. Yoder, C. F., S. P. Synnott and H. Salo, Orbits and masses of Saturn's coorbiting satellites, Janus and Epimetheus, *Astron. J.*, 98, 1875-1889, 1989.
122. Young, L. A. , C. B. Olkin, J. L. Elliot, D. J. Tholen and M. W. Buie, The Charon-Pluto mass ratio from MKO astrometry, *Icarus*, 108, 186-199, 1994.
123. Young, L. A. and R. P. Binzel, A new determination of radii and limb parameters for Pluto and Charon from mutual event data, *Icarus*, 108, 219-224, 1994.
124. Zharkov, V. N. and V. P. Trubitsyn, *Physics of Planetary interiors*, Pachart Publishing, Tucson, 388pp, 1978.